sequences followed by a loxP sequence was excised from PL451 plasmid (NCI), and inserted upstream of exon 2, generating the targeting vector "pMCS-DTA-FRTNeo-Aes^{f}" (Figure 7A). The integrity of the construct was verified by PCR and restriction digestion after introduction of the vector into Cre-expressing SW106 or Flpe-expressing SW105 strains (NCI). Then, the vector was introduced into D3a2 ES cells by homologous recombination and targeted ES clones were selected and karyotyped. Germ line-transmitted mice (*FRTNeo-Aes*$^{+/f}$) were generated and the PGK-Neo selection sequence was removed by crossing with actin promoter-driven FLPe transgenic mice (*TgaFlpe*) (Jackson Laboratory, ME), producing mice with a floxed *Aes* allele (*Aes*$^{+/f}$) (Figure S7B). We verified that homozygotes of these floxed *Aes* wild-types are viable, fertile and without any obvious phenotypes (data not shown). As shown in Figure 7B, we then crossed these *Aes*$^{+/f}$ female mice with *Apc*$^{+/\Delta716}$ males, and further crossed their compound heterozygotes with the compound heterozygotes obtained from crosses between *Aes*$^{+/f}$ males and Villin-Cre^{ERT2} transgenic (*TgvCre*^{ERT2}) females. At 3 weeks of age, the progeny compound mutant mice (*Apc*$^{+/\Delta716}$-*Aes*$^{f/f}$-*TgvCre*^{ERT2}) were treated with 4-hydroxytamoxifen (4HT; SIGMA) to activate Cre recombinase in the intestine-specific manner (el Marjou et al., 2004), generating *Apc*$^{+/\Delta716}$-*Aes*$^{\Delta ex2/\Delta ex2}$-*TgvCre*^{ERT2}, abbreviated as *Apc/Aes*.

Data Analysis

Data were analyzed by Student's t or chi-square tests and are presented as mean ± SD. P values <0.05 were considered significant.

ACCESSION NUMBERS

Microarray hybridization data have been deposited in the GEO database with accession code GSE12162.

SUPPLEMENTAL INFORMATION

Supplemental Information includes Supplemental Experimental Procedures, seven figures, and two movies and can be found with this article online at doi:10.1016/j.ccr.2010.11.008.

ACKNOWLEDGMENTS

We thank H. Kikuchi and Y. Mouri for excellent technical assistance, T. Honjo for plasmids and suggestions, T. Sudo for microarray analyses, Y. Yui and T. Tanaka for time-lapse microphotography, O. Takahashi for high-magnification fluorescence microphotography, S. Stifani for anti-panTLE antibody, H. Sasaki for Hedgehog reporters, T. Ishikawa, H. Miyoshi, A. Deguchi, S. Arimura, S. Yamashita, I. Okazaki, T. Okazaki, K. Okawa, C. Takahashi, T. Tomita, and Y. Morohashi for helpful discussions, S. Takahashi for microinjection of ES cells into blastcysts, N. Copeland, N. Jenkins, J. Takeda, and K. Yusa for biologicals and suggestions for the recombineering system. We also thank P. Vogt, To. Kitamura, M. Okabe, M. Kitagawa, and S. Kirkland for providing vectors pBSfi-AU1-TLE1, pMX-IRES-EGFP, pCX, Maml1 cDNA and HCA7 cells, respectively. This work was supported by grants from Ministry of Education, Culture, Sports, Science and Technology (MEXT), Japan, and by Jeannik M. Littlefield-AACR Grant in Metastatic Colon Cancer Research.

Received: June 7, 2010
Revised: September 17, 2010
Accepted: November 2, 2010
Published: January 18, 2011

REFERENCES

Artavanis-Tsakonas, S., Rand, M.D., and Lake, R.J. (1999). Notch signaling: cell fate control and signal integration in development. Science *284*, 770–776.

Brantjes, H., Roose, J., van de Wetering, M., and Clevers, H. (2001). All Tcf HMG box transcription factors interact with Groucho-related co-repressors. Nucleic Acids Res. *29*, 1410–1419.

Brinkmeier, M.L., Potok, M.A., Cha, K.B., Gridley, T., Stifani, S., Meeldijk, J., Clevers, H., and Camber, S.A. (2003). TCF and Groucho-related genes influence pituitary growth and development. Mol. Endocrinol. *17*, 2152–2161.

Chen, G., and Courey, A.J. (2000). Groucho/TLE family proteins and transcriptional repression. Gene *249*, 1–16.

Christofori, G. (2006). New signals from the invasive front. Nature *441*, 444–450.

Corbett, T.H., Griswold, D.P., Jr., Roberts, B.J., Peckham, J.C., and Schabel, F.M., Jr. (1975). Tumor induction relationships in development of transplantable cancers of the colon in mice for chemotherapy assays, with a note on carcinogen structure. Cancer Res. *35*, 2434–2439.

Detre, S., Saclani Jotti, G., and Dowsett, M. (1995). A "quickscore" method for immunohistochemical semiquantitation: validation for oestrogen receptor in breast carcinomas. J. Clin. Pathol. *48*, 876–878.

Downes, M., Ordentlich, P., Kao, H.-Y., Alvarez, J.G.A., and Evans, R.M. (2000). Identification of a nuclear domain with deacetylase activity. Proc. Natl. Acad. Sci. USA *97*, 10330–10335.

el Marjou, F., Janssen, K.P., Chang, B.H., Li, M., Hindie, V., Chan, L., Louvard, D., Chambon, P., Metzger, D., and Robine, S. (2004). Tissue-specific and inducible Cre-mediated recombination in the gut epithelium. Genesis *39*, 186–193.

Fidler, I.J. (2003). The pathogenesis of cancer metastasis: the "seed and soil" hypothesis revisited. Nat. Rev. Cancer *3*, 453–458.

Gasperowicz, M., and Otto, F. (2005). Mammalian Groucho homologs: redundancy or specificity? J. Cell. Biochem. *95*, 670–687.

Hoshino, H., Nishino, T.G., Tashiro, S., Miyazaki, M., Ohmiya, Y., Igarashi, K., Horinouchi, S., and Yoshida, M. (2007). Co-repressor SMRT and class II histone deacetylase promote Bach2 nuclear retention and formation of nuclear foci that are responsible for local transcriptional repression. J. Biochem. *141*, 719–727.

Hurlbut, G.D., Kankel, M.W., Lake, R.J., and Artavanis-Tsakonas, S. (2007). Crossing paths with Notch in the hyper-network. Curr. Opin. Cell Biol. *19*, 166–175.

Ilagan, M.X., and Kopan, R. (2007). Snapshot: Notch signaling pathway. Cell *128*, 1246.

Kao, H.Y., Ordentlich, P., Koyano-Nakagawa, N., Tang, Z., Downes, M., Kintner, C.R., Evans, R.M., and Kadesch, T. (1998). A histone deacetylase corepressor complex regulates the Notch signal transduction pathway. Genes Dev. *12*, 2269–2277.

Kashtan, H., Rabau, M., Mullen, J.B.M., Wong, A.H.C., Roder, J.C., Shpitz, B., Stern, H.S., and Gallinger, S. (1992). Intra-rectal injection of tumor cells: a novel animal model of rectal cancer. Surg. Oncol. *1*, 251–256.

Kato, H., Taniguchi, Y., Kurooka, H., Minoguchi, S., Sakai, T., Nomura-Okazaki, S., Tamura, K., and Honjo, T. (1997). Involvement of RBP-J in biological functions of mouse Notch1 and its derivatives. Development *124*, 4133–4141.

Kirkland, S.C. (1985). Dome formation by human colonic adenocarcinoma cell line (HCA-7). Cancer Res. *45*, 3790–3795.

Kitamura, T., and Taketo, M.M. (2007). Keeping out the bad guys: gateway to cellular target therapy. Cancer Res. *67*, 10099–10102.

Kitamura, T., Kometani, K., Hashida, H., Matsunaga, A., Miyoshi, H., Hosogi, H., Aoki, M., Oshima, M., Hattori, M., Takabayashi, A., et al. (2007). SMAD4-deficient intestinal tumors recruit CCR1^{+} myeloid cells that promote invasion. Nat. Genet. *39*, 467–475.

Lepourcelet, M., and Shivdasani, R.A. (2002). Characterization of a novel mammalian Groucho isoform and its role in transcriptional regulation. J. Biol. Chem. *277*, 47732–47740.

Liu, P., Jenkins, N.A., and Copeland, N.G. (2003). A highly efficient recombineering-based method for generating conditional knockout mutations. Genome Res. *13*, 476–484.

Lu, C., Bonome, T., Li, Y., Kmat, A.A., Han, L.Y., Schmandt, R., Coleman, R.L., Gershenson, D.M., Jaffe, R.B., Birrer, M.J., et al. (2007). Gene alterations identified by expression profiling in tumor-associated endothelial cells from invasive ovarian carcinoma. Cancer Res. *67*, 1757–1768.

Mailhos, C., Modlich, U., Lewis, J., Harris, A., Bicknell, R., and Ish-Horowicz, D. (2001). Delta4, an endothelial specific notch ligand expressed at sites of physiological and tumor angiogenesis. Differentiation *69*, 135–144.

Mallo, M., Gendron-Maguire, M., Harbison, M.L., and Gridley, T. (1995). Protein characterization and targeted disruption of *Grg*, a mouse gene related to the *groucho* transcript of the *Drosophila Enhancer of split* complex. Dev. Dyn. *204*, 338–347.

Milano, J., McKay, J., Dagenais, C., Foster-Brown, L., Pognan, F., Gadient, R., Jacobs, R.T., Zacco, A., Greenberg, B., and Ciaccio, P.J. (2004). Modulation of Notch processing by γ-secretase inhibitors causes intestinal goblet cell metaplasia and induction of genes known to specify gut secretory lineage differentiation. Toxicol. Sci. *82*, 341–358.

Oshima, M., Oshima, H., Kitagawa, K., Kobayashi, M., Itakura, C., and Taketo, M. (1995). Loss of *Apc* heterozygosity and abnormal tissue building in nascent intestinal polyps in mice carrying a truncated *Apc* gene. Proc. Natl. Acad. Sci. USA *92*, 4482–4486.

Oswald, F., Kostezka, U., Astrahantseff, K., Bourteele, S., Dillinger, K., Zechner, U., Ludwig, L., Wilda, M., Hameister, H., Knöchel, W., et al. (2002). SHARP is a novel component of the Notch/RBP-Jκ signalling pathway. EMBO J. *21*, 5417–5426.

Pinto, M., and Lobe, C.G. (1996). Products of the *grg* (*Groucho-related gene*) family can dimerize through the amino-terminal Q domain. J. Biol. Chem. *271*, 33026–33031.

Price, J.E. (2001). Xenograft models in immunodeficient animals: I. nude mice. In Methods in molecular medicine: Metastasis research protocols, *Volume II*, S.A. Brooks and U. Schumacher, eds. (Totowa, NJ: Humana Press), pp. 205–214.

Roose, J., Molenaar, M., Peterson, J., Kurenkamp, J., Brantjes, H., Moerer, P., van de Wetering, M., Destree, O., and Clevers, H. (1998). The *Xenopus* Wnt effector XTcf-3 interacts with Groucho-related transcriptional repressors. Nature *395*, 608–612.

Sancho, E., Batlle, E., and Clevers, H. (2004). Signaling pathways in intestinal development and cancer. Annu. Rev. Cell Dev. Biol. *20*, 695–723.

Schmidt, B. (2003). Aspartic proteases involved in Alzheimer's disease. ChemBioChem *4*, 366–378.

Shi, Y., Downes, M., Xie, W., Kao, H.Y., Ordentlich, P., Tsai, C.C., Hon, M., and Evans, R.M. (2001). Sharp, an inducible cofactor that integrates nuclear receptor repression and activation. Genes Dev. *15*, 1140–1151.

Smith, S.C., and Theodorescu, D. (2009). Learning therapeutic lessons from metastasis suppressor proteins. Nat. Rev. Cancer *9*, 253–264.

Steeg, P.S. (2006). Tumor metastasis: mechanistic insights and clinical challenges. Nat. Med. *12*, 895–904.

Takaku, K., Oshima, M., Miyoshi, H., Matsui, M., Seldin, M.F., and Taketo, M.M. (1998). Intestinal tumorigenesis in compound mutant mice of both *Dpc4* (*Smad4*) and *Apc* genes. Cell *92*, 645–656.

Taketo, M.M. (2006). Wnt signaling and gastrointestinal tumorigenesis in mouse models. Oncogene *25*, 7522–7530.

Taketo, M.M., and Edelman, W. (2009). Mouse models of colon cancer. Gastroenterology *136*, 780–798.

Tsutsumi, S., Kuwano, H., Morinaga, N., Shimura, T., and Asao, T. (2001). Animal model of para-aortic lymph node metastasis. Cancer Lett. *169*, 77–85.

van Es, J.H., Jay, P., Gregorieff, A., van Gijn, M.E., Jonkheer, S., Hatzis, P., Thiel, T.J., van den Born, M., Begthel, H., Brabletz, T., et al. (2005). Wnt signaling induces maturation of Paneth cells in intestinal crypts. Nat. Cell Biol. *7*, 381–386.

Wang, W.F., Wang, Y.G., Reginato, A.M., Plotkina, S., Gridley, T., and Olsen, B.R. (2002). Growth defect in Grg5 null mice is associated with reduced Ihh signaling in growth plates. Dev. Dyn. *224*, 79–89.

Weinberg, R.A. (2007). Moving out: invasion and metastasis. In The Biology of Cancer (New York: Garland Science), pp. 587–654.

Yabe, D., Fukuda, H., Aoki, M., Yamada, S., Takebayashi, S., Shinkura, R., Yamamoto, N., and Honjo, T. (2007). Generation of a conditional knockout allele for mammalian Spen protein Mint/SHARP. Genesis *45*, 300–306.

Zaczek, R., Olson, R.E., Seiffert, D.A., and Thompson, L.A. (1999). Compounds for inhibiting beta-amyloid peptide release and/or its synthesis. PCT Int. Appl. WO99/67221.

Zagouras, P., Stifani, S., Blaumueller, C.M., Carcangiu, M.L., and Artavanis-Tsakonas, S. (1995). Alterations in Notch signaling in neoplastic lesions of the human cervix. Proc. Natl. Acad. Sci. USA *92*, 6414–6418.

Zhu, X., Zhang, J., Tollkuhn, J., Ohsawa, R., Bresnick, E.H., Guillemot, F., Kageyama, R., and Rosenfeld, M. (2006). Sustained Notch signaling in progenitors is required for sequential emergence of distinct cell lineages during organogenesis. Genes Dev. *20*, 2739–2753.

Zimber, A., Nguyen, Q.D., and Gespach, C. (2004). Nuclear bodies and compartments: functional roles and cellular signaling in health and disease. Cell. Signal. *16*, 1085–1104.

Published OnlineFirst on January 11, 2011; DOI:10.1158/0008-5472.CAN-10-2842

Tumor and Stem Cell Biology

Cancer Research

Suppression of Colonic Polyposis by Homeoprotein CDX2 through its Nontranscriptional Function that Stabilizes $p27^{Kip1}$

Koji Aoki[1], Fumihiko Kakizaki[1], Hiromi Sakashita[2], Toshiaki Manabe[2], Masahiro Aoki[1], and Makoto M. Taketo[1]

Abstract

Caudal-related homeoprotein CDX2 is expressed in intestinal epithelial cells, in which it is essential for their development and differentiation. A tumor suppressor function is suggested by evidence that CDX2 levels are decreased in human colon cancer specimens and that an inactivating mutation of *Cdx2* in $Apc^{\Delta 716}$ mice markedly increases the incidence of colonic polyps. In this study, we investigated roles for transcriptional and nontranscriptional functions of CDX2 in suppression of colonic tumorigenesis. Mutagenic analysis of CDX2 revealed that loss of function stabilizes CDK inhibitor $p27^{Kip1}$ by a nontranscriptional but homeodomain-dependent mechanism that inhibits cyclin E-CDK2 activity and blocks G0/G1-S progression in colon cancer cells. $p27^{Kip1}$ stabilization was mediated by an inhibition of ubiquitylation-dependent proteolysis associated with decreased phosphorylation of Thr187 in $p27^{Kip1}$. siRNA-mediated knockdown of $p27^{Kip1}$ relieved the decrease in cyclin E-CDK2 activity and S-phase cell fraction elicited by CDX2 expression. Together, these results implicate a nontranscriptional function of CDX2 in tumor suppression mediated by $p27^{Kip1}$ stabilization. Up to approximately 75% of low-CDX2 human colon cancer lesions show reduced levels of $p27^{Kip1}$, whereas approximately 68% of high-CDX2 lesions retain expression of $p27^{Kip1}$. These results show that low levels of CDX2 accelerate colon tumorigenesis by reducing $p27^{Kip1}$ levels. *Cancer Res; 71(2); 593–602. ©2011 AACR.*

Introduction

Homeobox transcription factor CDX2 is a mammalian homologue of *Drosophila* caudal that induces the anteroposterior axis (1, 2). In mammalian embryogenesis, CDX2 is essential for self-renewal of the trophoblast cells (3), anteroposterior patterning of the vertebrae, and development of the intestines (4, 5). In adults, CDX2 is expressed specifically in the intestinal epithelium (Fig. 1A; refs. 1, 6), and induces expression of digestive enzymes, adhesion proteins, and transporters (7). In mice, homozygous *Cdx2* mutation causes embryonic lethality whereas the heterozygotes show developmental anomalies, including gastrointestinal hamartomas (4, 5). Consistently, development and differentiation of the intestinal epithelial cells are blocked by homozygous deletion of *Cdx2* in developing intestines (8, 9). These results indicate that CDX2 plays key roles in development and differentiation of colonic epithelial cells.

The levels of CDX2 are reduced in most human colon cancer tissues (10, 11), and in colonic polyps of the $Apc^{+/\Delta 716}$ ($Apc^{+/-}$) mutant mice, a model for human familial adenomatous polyposis (12, 13). The $Cdx2^{+/-}$ mutation increases the colonic polyp number approximately 6 times in $Apc^{+/-}$ mice (Fig. 1B; ref. 12), and accelerates colonic tumorigenesis induced by azoxymethane treatment (14). In mice, and in human and rat colon cancer cell lines, reduced levels of CDX2 stimulate G1-S cell-cycle progression and increase chromosomal instability (12). These results suggest that reduced levels of CDX2 accelerate colonic tumorigenesis. However, the mechanism has been unknown, and its target gene that can suppress tumorigenesis unidentified. To investigate its transcriptional and possibly nontranscriptional functions in the suppression of colonic tumorigenesis, we have performed a mutagenesis analysis of the CDX2 homeodomain (HD) and deletion studies of the protein. We have found that CDX2 has a HD-mediated, but nontranscriptional activity that is sufficient for blocking G1-S progression in the colonic epithelial cell cycle through stabilization of $p27^{Kip1}$ protein. These results suggest a novel nontranscriptional mechanism through which CDX2 suppresses colonic tumorigenesis.

Authors' Affiliations: [1]Department of Pharmacology, Graduate School of Medicine, Kyoto University, and [2]Laboratory of Diagnostic Pathology, Kyoto University Hospital, Kyoto, Japan.

Note: Supplementary data for this article are available at Cancer Research Online (http://cancerres.aacrjournals.org/).

Corresponding Author: Makoto Mark Taketo, Department of Pharmacology, Graduate School of Medicine, Kyoto University, Yoshida-Konoé-cho, Sakyo-ku, Kyoto 605-8501, Japan. Phone: 81-75-753-4391; Fax: 81-75-753-4402. E-mail: taketo@mfour.med.kyoto-u.ac.jp

doi: 10.1158/0008-5472.CAN-10-2842

Published OnlineFirst on January 11, 2011; DOI:10.1158/0008-5472.CAN-10-2842

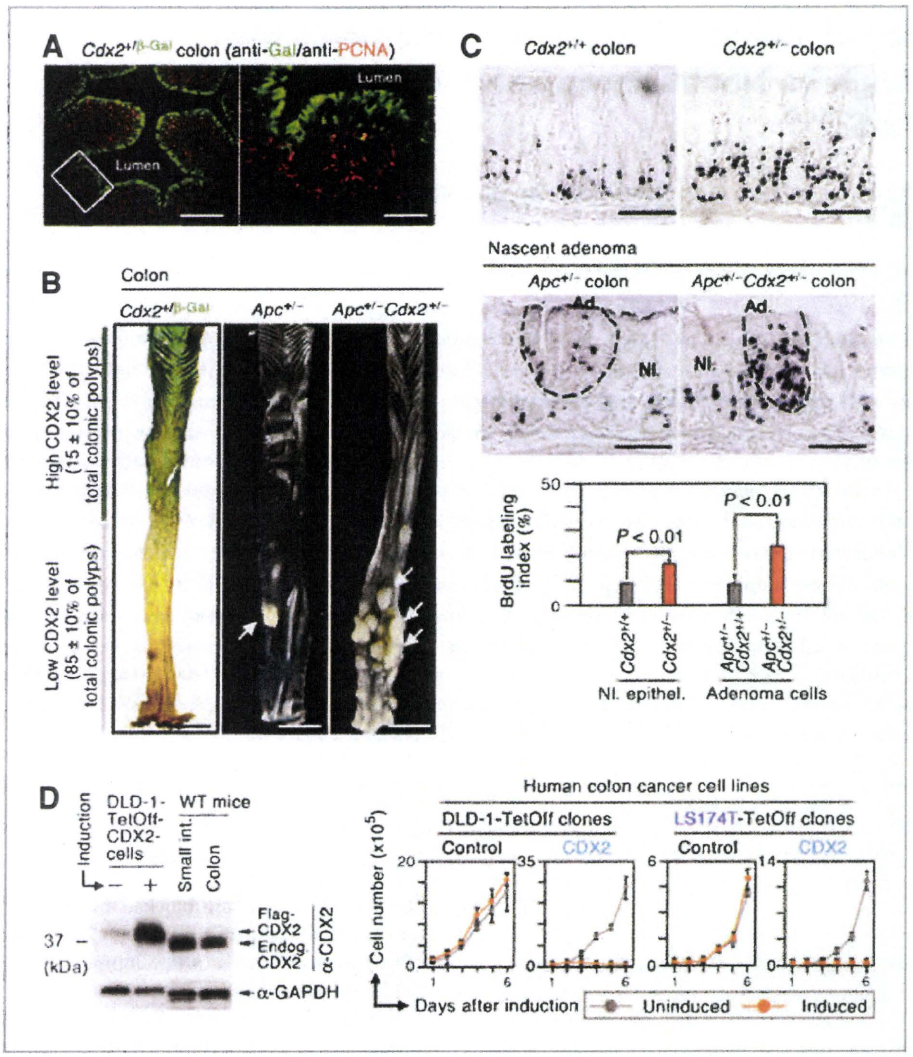

Figure 1. CDX2 blocks cell proliferation of normal, adenoma, and carcinoma epithelia of colon. A, relationship between CDX2 expression (green) and proliferation (red) in colonic epithelial cells in a cross section at low magnification (left). The colon of *Cdx2*–β-Gal (β-galactosidase) knock-in mice ($Cdx2^{+/\beta\text{-Gal}}$) were stained with antibodies for β-Gal (green) and PCNA (a marker for cell proliferation, red), simultaneously. Right, a higher magnification of the boxed area in the left. Magnification bars, 400 μm (left) and 100 μm (right). B, representative photographs of LacZ-stained $Cdx2^{+/\beta\text{-Gal}}$ colon (left), and nonstained colons of $Apc^{+/-}$ (center) and $Apc^{+/\Delta 716}Cdx2^{+/\beta\text{-Gal}}$ ($Apc^{+/-}Cdx2^{+/-}$; right). Scale bars, 1 cm. Note that approximately 85% of polyps in $Apc^{+/-}$ and $Apc^{+/-}Cdx2^{+/-}$ were found in the distal region where the level of CDX2 was lowest. Polyp distribution with SD were from 4 $Apc^{+/-}$ and 4 $Apc^{+/-}Cdx2^{+/-}$ mice at 10 weeks of age. Arrows point to representative colonic polyps in the large-size class. C, representative photographs of colonic epithelial cells labeled with BrdU in wild-type ($Cdx2^{+/+}$) and $Cdx2^{+/-}$ mice (top), and those of adenoma cells in nascent polyps of $Apc^{+/-}$ and $Apc^{+/-}Cdx2^{+/-}$ mice (middle) at 10 weeks of age. Quantified data from 3 mice are shown with SD (bottom). Nl., normal colonic mucosa; Ad., adenoma cells; Epithel., epithelial cells. Magnification bars, 100 μm. D, induction of Flag-tagged CDX2 in DLD-1–TetOff cells analyzed by Western blotting (WB; left), compared with that in lysates prepared from intestines (int.) of wild-type mouse. Glyceraldehyde 3 phosphate dehydrogenase (GAPDH) was used as a loading control. Note that induced Flag-CDX2 shows slower migration than endogenous (endog.) CDX2, due to its Flag tag. Proliferation profiles of DLD-1–TetOff and LS174T–TetOff cell clones that induced expression of CDX2 are shown with SD, compared with uninduced cells (right).

Materials and Methods

BrdU labeling, X-gal staining, determination of polyp distribution, and human tissue samples

The $Apc^{+/-}$, $Cdx2^{+/\beta\text{-Gal}}$ ($Cdx2^{+/-}$), and $Apc^{+/-}Cdx2^{+/-}$ mice have been described previously (5, 12, 13). Bromodeoxyuridine (BrdU) labeling and X-gal staining were carried out as described previously (5, 12). All animal experiments were approved by the Animal Care and Use Committee of Kyoto University. Colonic polyps in the $Apc^{+/-}$ and $Apc^{+/-}Cdx2^{+/-}$ mice (4 mice at the age of 10 weeks, respectively) were scored as described previously (12). Human tissue samples and

Published OnlineFirst on January 11, 2011; DOI:10.1158/0008-5472.CAN-10-2842

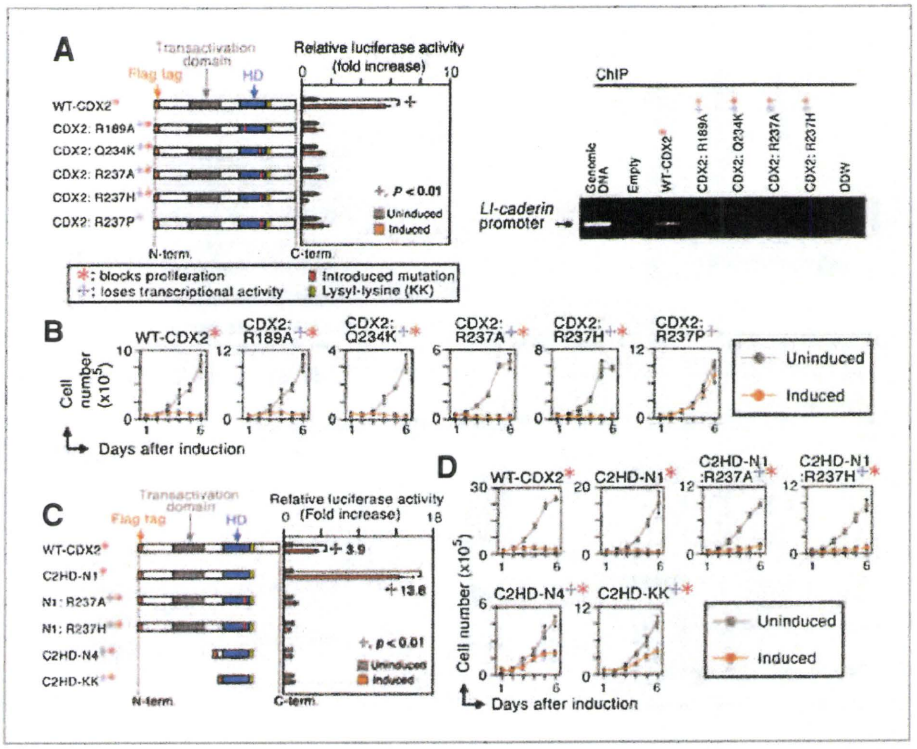

Figure 2. Nontranscriptional activity of CDX2 in N-terminal (N-term.) and homeobox domains is sufficient to block cell proliferation. A, schematic representation of transcription-defective CDX2 mutant proteins (left). Transcriptional activities of the respective mutant CDX2 proteins were determined on day 2 of induction in DLD-1–TetOff clones, using a luciferase reporter carrying a promoter region of the *LI-cadherin* gene (left). The activities are shown with SD. Lack of DNA-binding activity of CDX2 mutant proteins was also analyzed by chromatin immunoprecipitation assay (ChIP) for the *LI-cadherin* gene promoter (right). Genomic DNA was used as a positive control. C-term, C-terminal. B, proliferation profiles of DLD-1–TetOff cells on induction of transcription-defective CDX2 mutant proteins, compared with uninduced cells. The mean cell numbers are shown with SD. C, schematic representation of CDX2 deletion mutant proteins (left). Transcriptional activities of the respective mutant CDX2 proteins were determined on day 2 of induction in DLD-1–TetOff clones, using a luciferase reporter carrying a promoter region of the *LI-cadherin* gene (right). The activities are shown with SD. Right, numbers indicate relative ratios of the induced to the uninduced activities. D, proliferation profiles of DLD-1–TetOff cells on induction of CDX2 deletion mutant proteins, compared with uninduced cells. The mean cell numbers are shown with SD.

immunohistochemical analysis are described in Supplementary Data.

TetOff system and introduction of small interfering RNA into TetOff cells

TetOff cells were generated, using a pTetOff vector (Clontech). CDX2 and its mutants were expressed in the respective stable TetOff cell clones, using a pTRE-Tight vector (Clontech). Introduction of small interfering RNA duplexes (siRNA) into TetOff cells and siRNA used in this study, and cell-proliferation assay are described in Supplementary Data.

Mutagenesis of CDX2 HD and construction of CDX2 deletion mutants

Mutagenesis of the CDX2 HD was carried out using QuickChange II Site-Directed Mutagenesis Kit (Stratagene), and confirmed by sequencing. Deletion mutants of CDX2 were constructed by PCR. Sequences of oligonucleotides used for the mutagenesis and for construction of the deletion mutants are provided in Supplementary Data. Construction of luciferase reporters and chromatin immunoprecipitation analysis are also described in Supplementary Data (15).

Immunoprecipitation, Western blotting, and cycloheximide chase

Analyses of the $p27^{Kip1}$ complex and its subcelluar localization are described in Supplementary Data. For analysis of the $p27^{Kip1}$ ubiquitylation, cells were treated with 10 μmol/L of MG132 (Sigma-Aldrich) for 12 hours.

For analysis of $p27^{Kip1}$ protein stabilization, cells were treated with 100 μg/mL of cycloheximide (CHX; Sigma-Aldrich). Quantitative RT-PCR analysis for the *CDKN1B* mRNA is also described in Supplementary Data.

Statistical analysis

Statistical analyses were carried out by the Student's t test to compare the mean (Figs. 1, 2, and 4), or by the χ^2 test to compare the CDX2 and $p27^{Kip1}$ levels in human colon cancer specimens (Fig. 6), using JMP software (SAS Institute Japan). $P < 0.05$ was considered significant.

Published OnlineFirst on January 11, 2011; DOI:10.1158/0008-5472.CAN-10-2842

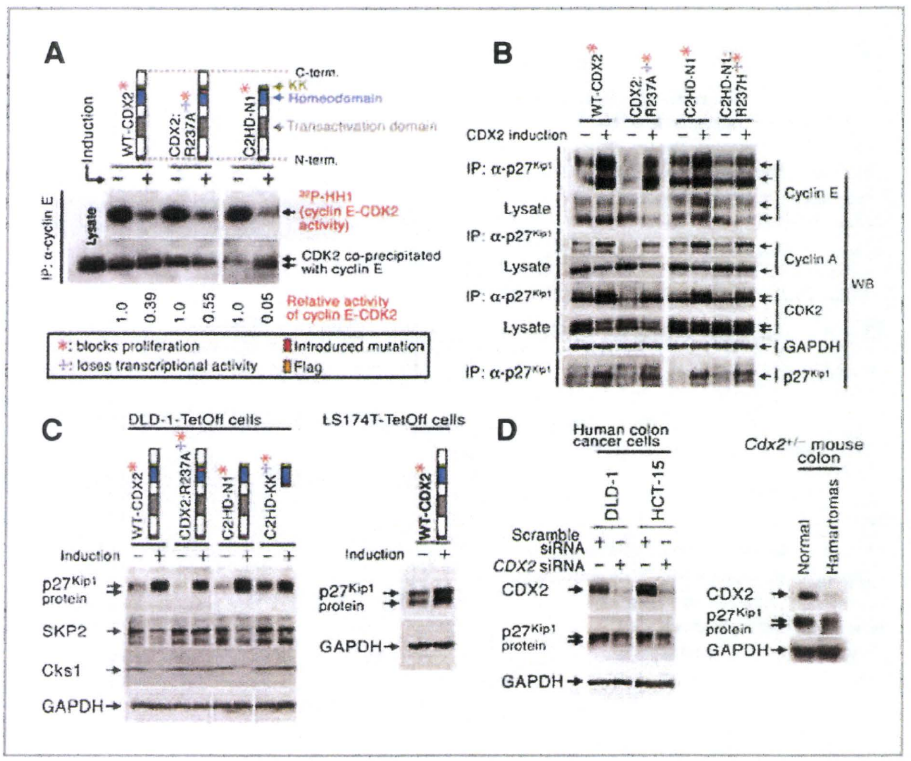

Figure 3. CDX2 increases amounts of $p27^{Kip1}$ protein and cyclin-CDK2/$p27^{Kip1}$ complex. A, kinase activity of CDK2 coimmunoprecipitated with cyclin E (IP; anti-cyclin E) on histone H1 (HH1) substrate on day 2 of induction of wild-type or mutant CDX2 in DLD-1–TetOff cells, analyzed by *in vitro* kinase assay. The ^{32}P incorporation into HH1 is shown (top). The level of CDK2 coimmunoprecipitated with cyclin E was also analyzed by Western blotting (bottom). The relative kinase activities of cyclin E-CDK2 are shown beneath the gel photo. The faster-migrating band of CDK2 corresponds to the protein phosphorylated only at T160 that is essential for its activation, whereas the slower band represents CDK2 phosphorylated at inhibitory phosphorylation sites Y14 and T15 (41). C-term, C-terminal; N-term, N-terminal. B, amounts of cyclin E, cyclin A, and CDK2 coimmunoprecipitated with $p27^{Kip1}$ analyzed by immunoprecipitation assay (IP), on day 2 of induction of wild-type CDX2 or its mutants in the DLD-1–TetOff clones. Amounts of the cyclins and CDK2 coimmunoprecipitated with $p27^{Kip1}$, and their lysate levels were analyzed by Western blotting (WB). Glyceraldehyde 3 phosphate dehydrogenase (GAPDH) was used as a loading control, and precipitated $p27^{Kip1}$ is also shown. C, amounts of $p27^{Kip1}$, SKP2, and Cks1 proteins on day 2 of induction of wild-type or mutant CDX2 in DLD-1–TetOff (left) and in LS174T–TetOff cell clones (right), analyzed by Western blotting. GAPDH was used as a loading control. Double bands of $p27^{Kip1}$ protein have been described (42). D, amount of $p27^{Kip1}$ protein on day 2 after introduction of siRNA against *CDX2* in human colon cancer cell lines DLD-1 and HCT-15, analyzed by Western blotting (left). Reduced level of CDX2 is shown on the top (left). Amount of $p27^{Kip1}$ protein in colonic hamartomas of the $Cdx2^{+/-}$ mutant mice was analyzed by Western blotting (right). GAPDH was used as a loading control. Note essentially absent CDX2 in the hamartomas (right, top). Normal, the lysate derived from the surrounding normal mucosa.

Results

CDX2 blocks cell proliferation of normal, adenoma and carcinoma epithelia of colon

In the colonic epithelium, CDX2 was expressed strongly in the nonproliferating differentiated cells, whereas its level in the proliferating cells was much lower (Fig. 1A; ref. 6). The $Cdx2^{+/-}$ mutation increased proliferation of normal colonic epithelial cells by approximately 2 times (Fig. 1C, top) and of adenoma cells by approximately 3 times (Fig. 1C, middle). These results suggest that CDX2 normally suppresses proliferation of normal and adenoma epithelial cells of the colon. Consistently, most colonic polyps were found in the distal region where the level of CDX2 was low, in both $Apc^{+/-}$ and $Apc^{+/-}Cdx2^{+/-}$ mutant mice (Fig. 1B; 79 ± 8% and 92 ± 8%, respectively; mean ± SD).

To investigate the mechanism by which CDX2 suppressed the proliferation, we constructed doxycycline-controlled "Tet-Off–CDX2" cell clones, in which CDX2 was induced at levels comparable to those in the normal intestines (Fig. 1D, left). As test cells, we chose near-diploid human colon cancer lines DLD-1 and LS174T, which were used as models for the intestinal progenitor cells (16) and expressed low levels of CDX2 (Fig. 1D, left). In these cell lines, Wnt signaling is activated through mutations in the *APC* and β-catenin genes, respectively. In addition, both Ras and phosphatidylinositol-3 kinase (PI3K)-Akt signaling pathways are also activated by mutations in *KRAS* and *PIK3CA* genes (17), whereas p53 is mutated only in DLD-1 cells.

As expected, induction of CDX2 in the TetOff cells caused 2 to 3 times higher transcriptional activities as determined by luciferase reporters carrying promoters for the *LI-cadherin*

Published OnlineFirst on January 11, 2011; DOI:10.1158/0008-5472.CAN-10-2842

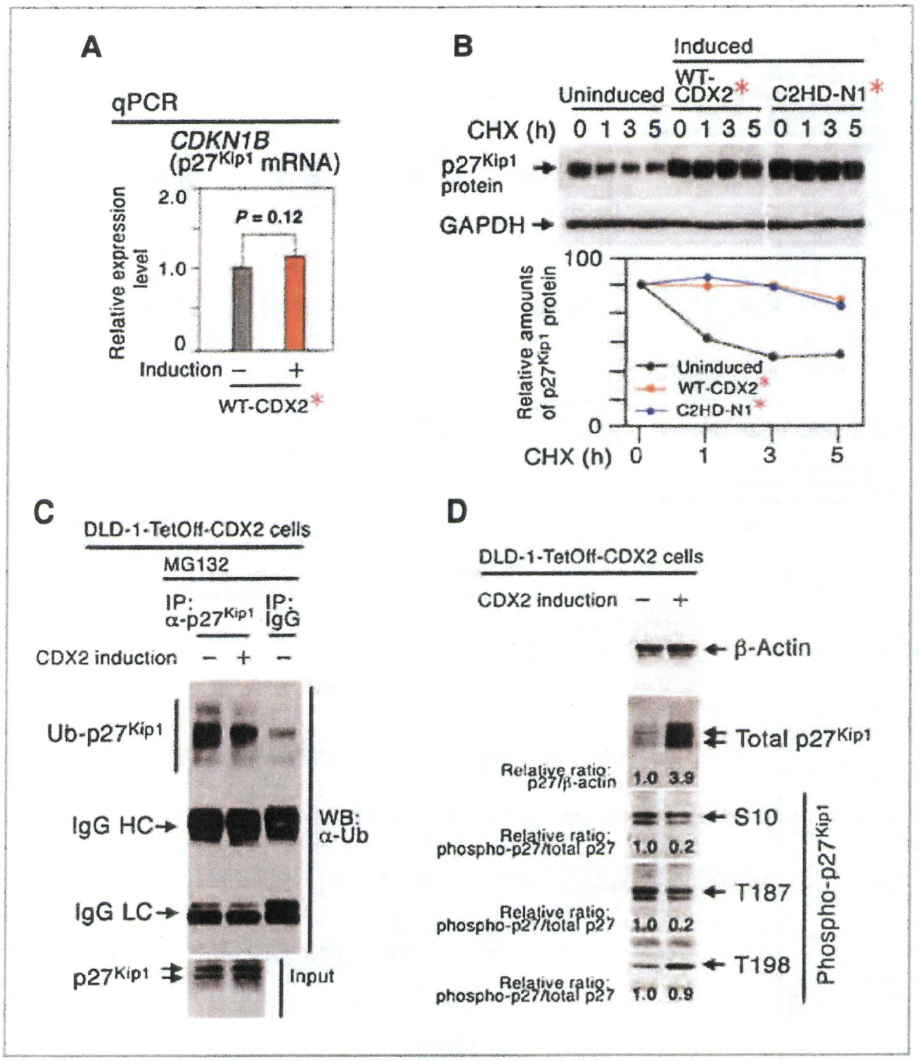

Figure 4. CDX2 stabilizes $p27^{Kip1}$ protein by blocking its ubiquitylation. A, amount of $p27^{Kip1}$ (*CDKN1B*) mRNA on day 2 of induction of wild-type CDX2 in DLD-1–TetOff cell clones, analyzed by quantitative PCR (qPCR). B, amount of $p27^{Kip1}$ protein at the indicated hours after treatment with cycloheximide (CHX) on induction of wild-type CDX2 or C2HD-N1 protein, analyzed by Western blotting (top). GAPDH was used as a loading control. Quantified data are shown in bottom. C, the level of polyubiquitylated $p27^{Kip1}$, analyzed by Western blotting, on expression of CDX2 in DLD-1 cells. DLD-1–TetOff cells were treated with 10 μmol/L of MG132 for 12 hours to inhibit proteasome activity. $p27^{Kip1}$ in the cell lysate was immunoprecipitated using an antibody for $p27^{Kip1}$, and the level of polyubiquitylated $p27^{Kip1}$ was analyzed by Western blotting, using an antibody for ubiquitin. D, phosphorylation levels of $p27^{Kip1}$ at S10, T187, and T189 analyzed by Western blotting, on expression of CDX2 in DLD-1–TetOff cells. β-Actin was used as a loading control. Numbers for S10, T187, and T189 phosphorylation indicate relative ratios of the phosphorylated $p27^{Kip1}$ to the total $p27^{Kip1}$, whereas those for total $p27^{Kip1}$ indicate relative levels of $p27^{Kip1}$ to β-actin.

and *HEPH* genes (Supplementary Fig. S1A), both controlled by CDX2 (18, 19). Importantly, induction of CDX2 arrested the TetOff cells in the G0/G1 cell-cycle phase and suppressed proliferation (Fig. 1D, right; Supplementary Figs. S1B and S2A). The same results were obtained with mouse colon cancer cells Colon26, in which Wnt signaling was not activated (Supplementary Fig. S1C and D). Consistently, knockdown of endogenous CDX2 expression increased the S-phase fraction by approximately 10% (Supplementary Fig. S2B and C). These results suggest that CDX2 suppresses proliferation of not only normal and adenoma epithelia but also colon cancer cells by blocking G0/G1-S progression.

Nontranscriptional activity of CDX2 in N-terminal and homeobox domains is sufficient to block cell proliferation

Because homeobox proteins function as transcription factors through their HDs (20), we investigated whether CDX2 blocked cell proliferation through its transcriptional activity. To this end, we constructed transcription-defective CDX2 mutants that contained point mutations in the HD (Fig. 2A, left). Mutations R189A, R237A, R237H, and R237P have been reported to eliminate the binding activity of HD to DNA, whereas Q234K alters its DNA-binding specificity (21). These HD mutations (R189A, Q234K, R237A, R237H, and R237P) lost the transcriptional activation for CDX2-target gene promoters (Fig. 2A, left, *LI-cadherin* gene promoter; Supplementary Fig. S3A, *HEPH* promoter), although all mutant proteins were stable, and localized predominantly to the nucleus (Supplementary Fig. S4A and B). Consistently, the HD mutations lost DNA-binding activity for the CDX2-target gene promoters (Fig. 2A, right, *LI-cadherin* gene promoter; Supplementary Fig. S3B, *sucrase isomaltase* promoter). Surprisingly, the transcription-defective CDX2 mutants (R189A, Q234K, R237A, and R237H) retained similar blocking activities on cell proliferation to that of the wild type (WT; Fig. 2B; Supplementary

Published OnlineFirst on January 11, 2011; DOI:10.1158/0008-5472.CAN-10-2842

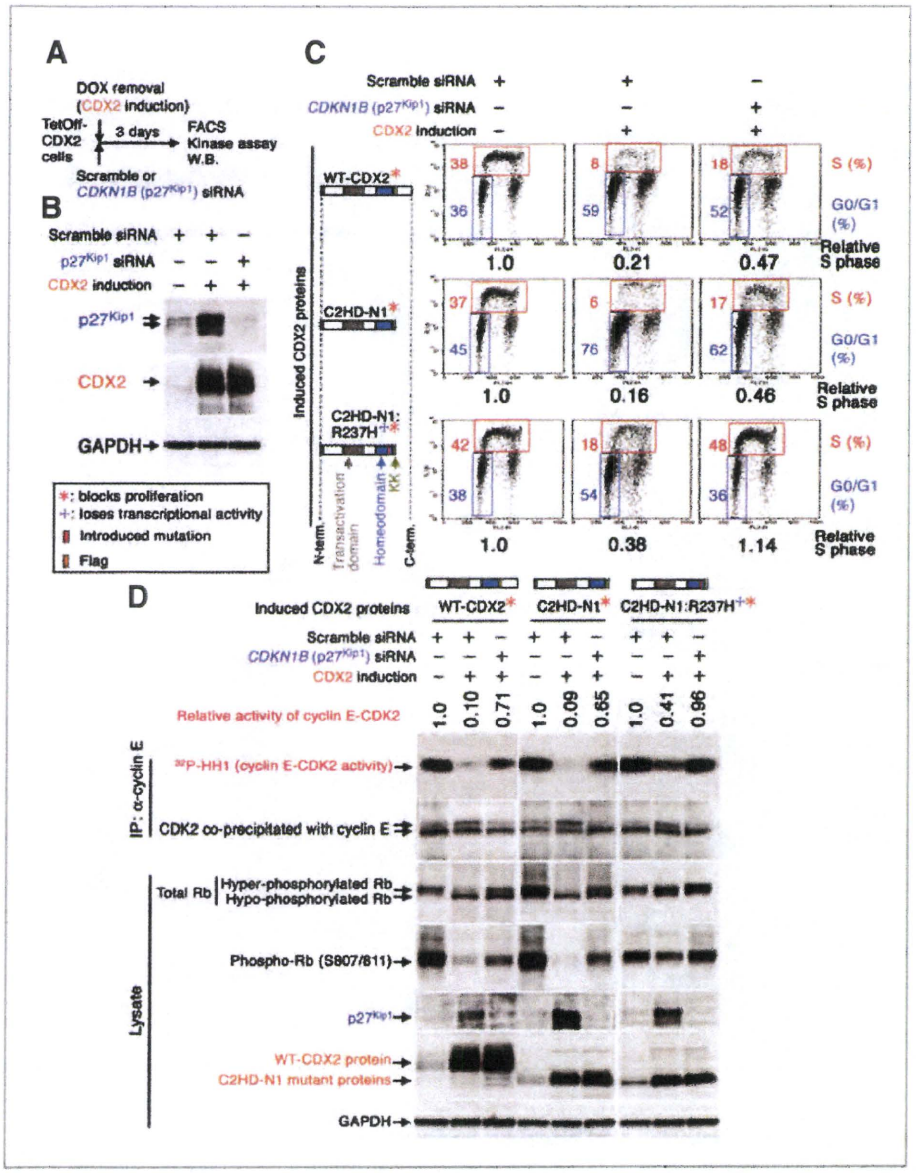

Figure 5. $p27^{Kip1}$ is critical for CDX2 to block cell-cycle progression. A and B, suppression of $p27^{Kip1}$ expression on day 3 after introduction of *CDKN1B* ($p27^{Kip1}$) siRNA simultaneously with expression of wild-type CDX2 in TetOff cells (A; schematic experimental strategy), analyzed by Western blotting (B, top). Band for CDX2 is also shown in the middle (B). GAPDH was used as a loading control (B, bottom). C, cell-cycle profiles on day 3 after introduction of $p27^{Kip1}$ siRNA and simultaneous expression of wild-type CDX2 (top), mutant C2HD-N1 (middle), or transcription-defective mutant C2HD-N1:R237H (bottom) in TetOff cells, analyzed by flow cytometry. D, kinase activity of cyclin E-CDK2 (IP; anti-cyclin E) on histone H1 (HH1) substrate on day 3 after introduction of $p27^{Kip1}$ siRNA and simultaneous expression of WT-CDX2 (left), C2HD-N1 (center), or C2HD-N1:R237H (right) in TetOff cells, analyzed by *in vitro* kinase assay. Incorporation of ^{32}P into HH1 is shown (top). The level of CDK2 coimmunoprecipiated with cyclin E was also analyzed by Western blotting. The relative kinase activities of cyclin E-CDK2 are shown above the photo. Phosphorylation level of Rb in the TetOff cell lysate on day 3 was also analyzed by Western blotting.

Fig. S3C). Importantly, these results suggest that both transcriptional and DNA-binding activities are dispensable for blocking proliferation by CDX2. On the contrary, another mutation R237P suppressed inhibition of cell proliferation by CDX2 (Fig. 2B), suggesting that HD was essential for the block of proliferation.

To localize in CDX2 the domains responsible for blocking cell proliferation, we then constructed deletion mutants "C2HDs" that retained its HD (Fig. 2C). Mutant C2HD-KK contained HD and its C-terminally adjacent lysyl-lysine (KK; Fig. 2C). Mutants C2HD-N1 and -N4 contained HD with C-terminal KK, and N-terminal extensions (Fig. 2C). Because mutant C2HD-N1 retained the transactivation domain (22) and activated the *LI-cadherin* and *HEPH* promoters, we also constructed its transcription-defective derivatives that carried HD mutations R237A and R237H (C2HD-N1:R237A and -N1:R237H, respectively; Fig. 2C). All C2HD proteins were expressed stably in DLD-1 cells (Supplementary Fig. S5A and B), whereas we failed to construct cells expressing CDX2 deletion mutant proteins lacking HD, due to their instability *in vivo* (data not shown). Like WT-CDX2 and C2HD-N1, cell proliferation was still blocked by induction of C2HD-N1 derivatives that lacked both the C-terminal domain and transcriptional activity (C2HD-N1:R237A and -N1:R237H; Fig. 2C and D; Supplementary Fig. S6A and B). These results indicate that CDX2 C-terminal domain as well as

Published OnlineFirst on January 11, 2011; DOI:10.1158/0008-5472.CAN-10-2842

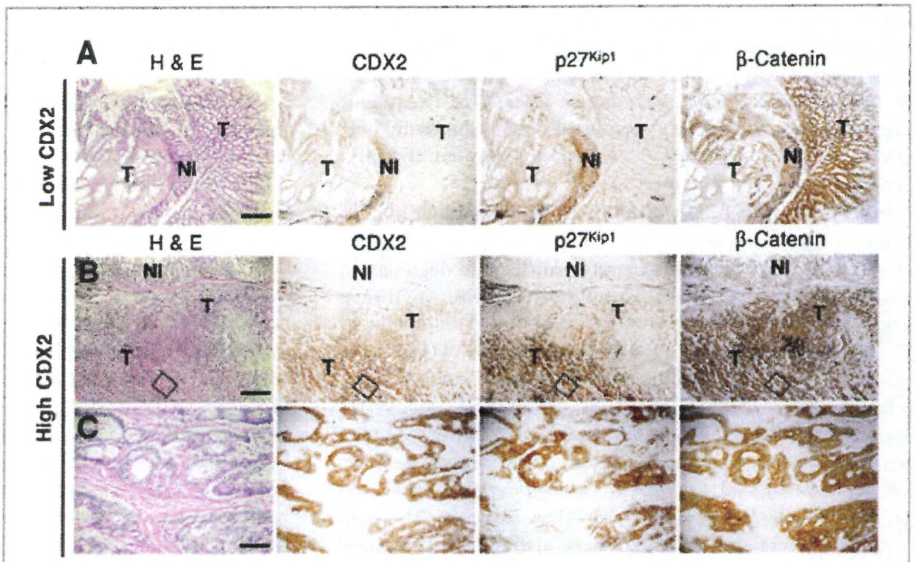

D

Correlation between CDX2 and $p27^{Kip1}$ protein levels in human colon cancer tissues

Variables		Low CDX2	High CDX2	P (χ^2 test)
		n = 28	n = 31	
Tumor stage	I, II	12 (43%)	16 (52%)	
	III, IV	16 (57%)	15 (48%)	0.50
$p27^{Kip1}$ level	Low	21 (75%)	10 (32%)	
	High	7 (25%)	21 (68%)	<0.001

Figure 6. Correlation between CDX2 and $p27^{Kip1}$ levels in human colon cancer tissues. A–C, representative photographs for the low-CDX2 (A) and high-CDX2 (B and C) colon cancer tissues. Tissues were stained with hematoxylin and eosin, or antibodies for CDX2, $p27^{Kip1}$, or β-catenin. C, higher magnifications of insets in B, respectively. T, tumor tissue; NI, normal mucosa. β-Catenin was used as a positive control for immunohistochemistry. Note that the level of β-catenin was increased in the tumor tissue compared with that in normal mucosa. Bars, 1 mm. D, correlation between the CDX2 and $p27^{Kip1}$ levels in 59 human colon cancer specimens. P values were obtained by the $\chi 2$ test.

transcriptional activity was dispensable for the proliferation block. Although cell proliferation was also blocked by C2HD-KK and C2HD-N4 (Fig. 2D), the effect was only partial, suggesting that the HD alone was insufficient, and its N-terminal domain was needed for the full activity of CDX2.

CDX2 increases amounts of $p27^{Kip1}$ protein and cyclin-CDK2/$p27^{Kip1}$ complex

Progression from the G1 to S phase is positively regulated by the cyclin E-CDK2 complex (23). We found that the cellular cyclin E-CDK2 kinase activity was decreased by expression of WT-CDX2 or its mutants (CDX2:R237A and C2HD-N1), as assayed by histone H1 (HH1) phosphorylation (Fig. 3A; total CDK2 activity, Supplementary Fig. S7A, left). At the same time, induction of WT-CDX2 or mutant CDX2:R237A increased the amounts of cyclin E, cyclin A, and CDK2 coimmunoprecipitated with $p27^{Kip1}$, whereas the induction reduced the lysate levels of cyclin A and CDK2 (Fig. 3B). Induction of WT-CDX2 or CDX2:R237A also increased the level of total $p27^{Kip1}$ protein in the lysate of DLD-1 cells (Fig. 3C, left; for quantified data, Supplementary Fig. S7A, right, by approximately 3 times), without affecting the subcellular localizations of the cyclins, CDK2 and $p27^{Kip1}$ (Supplementary Fig. S7B, left). Also, in LS174T cells, the level of $p27^{Kip1}$ was increased on expression of CDX2 (Fig. 3C, right). These results suggest that expression of CDX2 increases the amounts of cyclin E-CDK2/$p27^{Kip1}$ and cyclin A-CDK2/$p27^{Kip1}$ complexes through raising the level of $p27^{Kip1}$. Consistently, the $p27^{Kip1}$ protein level was decreased in the reduced-CDX2 cells (by approximately 40%; Fig. 3D, left) and *Cdx2*$^{+/-}$ colonic hamartomas where CDX2 was essentially absent (by approximately 90%; Fig. 3D, right).

Also, by expression of deletion mutant C2HD-N1 and its transcription-deficient derivatives (C2HD-N1:R237H and -N1:R237A), the level of $p27^{Kip1}$ in cell lysates was increased, as well as those of cyclin E- and cyclin A-CDK2/$p27^{Kip1}$ complexes (Fig. 3B and C; Supplementary Fig. S7B, right). On the contrary, mutation R237P suppressed increase in the level of $p27^{Kip1}$ (Supplementary Fig. S7C). These results show that the N-terminal and HD in CDX2 are sufficient for increasing the $p27^{Kip1}$ level and blocking proliferation.

Expression of CDX2 stabilizes $p27^{Kip1}$ by blocking its ubiquitylation

In contrast to the increased level of $p27^{Kip1}$ protein (Fig. 3C), its mRNA (*CDKN1B*) level remained unchanged on induction of CDX2 (Fig. 4A), suggesting that CDX2 stabilized $p27^{Kip1}$

Published OnlineFirst on January 11, 2011; DOI:10.1158/0008-5472.CAN-10-2842

protein. To test this possibility, we treated CDX2-induced cells with CHX, an inhibitor of protein translation. In the CDX2-uninduced control cells, the level of $p27^{Kip1}$ protein decreased by approximately 50% in 3 hours after CHX treatment (Fig. 4B). However, the level decreased only by approximately 10% on induction of WT-CDX2 or C2HD-N1 protein (Fig. 4B), showing that CDX2 stabilized $p27^{Kip1}$ protein.

Stability of $p27^{Kip1}$ is controlled by SKP2 through ubiquitylation-mediated proteolysis (24–29). Because polyubiquitylated $p27^{Kip1}$ is detectable when its proteasomal degradation is inhibited, we treated CDX2-induced cells with MG132, a proteasome inhibitor. Notably, the level of polyubiquitylated $p27^{Kip1}$ was decreased on expression of CDX2 (Fig. 4C), whereas those of polyubiquitylated cyclins E and A, other SKP2 targets, were increased (Supplementary Fig. S7D). Because these results suggested that the $p27^{Kip1}$ ubiquitylation was specifically suppressed by CDX2 expression, we further investigated the $p27^{Kip1}$ phosphorylation that can control its ubiquitylation (24–31). The ratios of S10- and T187-phosphorylated $p27^{Kip1}$ to the total $p27^{Kip1}$ were reduced significantly to approximately 20% on induction of CDX2, whereas that of T198 was not affected (Fig. 4D). The phosphorylation of $p27^{Kip1}$ at T187 reduces the stability of $p27^{Kip1}$ through accelerating the ubiquitylation-mediated degradation, whereas that of S10 stabilizes $p27^{Kip1}$ (30–33). Thus, it is likely that the reduced level of the T187 phosphorylation is a main cause of the $p27^{Kip1}$ stabilization on expression of CDX2.

$p27^{Kip1}$ is critical for CDX2 to block cell-cycle progression

To investigate further the role of $p27^{Kip1}$ in the CDX2-mediated proliferation block, we simultaneously induced CDX2, and suppressed $p27^{Kip1}$ expression by introducing siRNA against *CDKN1B* ($p27^{Kip1}$ siRNA) into the TetOff–CDX2 cells (Fig. 5A and B). Notably, knocking down $p27^{Kip1}$ completely prevented the decrease in the S-phase fraction on expression of C2HD-N1:R237H (transcription-defective C2HD-N1 mutant; Fig. 5C, bottom; compare center and right). These results show that the increased level of $p27^{Kip1}$ is essential for CDX2 to block G0/G1-S phase progression. Consistently, reducing the level of $p27^{Kip1}$ completely blocked the decrease in the cyclin E–associated CDK2 activity on expression of C2HD-N1:R237H (Fig. 5D; right, top) or C2HD-N1:R237A (Supplementary Fig. S8). The reduced level of $p27^{Kip1}$ in C2HD-N1:R237H–induced cells also blocked the decrease in the phosphorylation level of retinoblastoma protein (Rb; Fig. 5D, right), an endogenous target by cyclin E-CDK2 (34, 35). These results collectively indicate that CDX2 stabilizes $p27^{Kip1}$ through its nontranscriptional activity, which causes inhibition of cyclin E-CDK2 and blocks cell proliferation.

Furthermore, reducing the level of $p27^{Kip1}$ partially suppressed the decrease in the S-phase fraction on expression of WT-CDX2 or C2HD-N1 that retained transcriptional activity (Fig. 5C, top and middle). Consistently, the reduced level of $p27^{Kip1}$ partially suppressed the decreases in cyclin E-CDK2 activity and phosphorylation level of Rb (Fig. 5D, left and center). These results verify that $p27^{Kip1}$ is critical for CDX2 to block cell-cycle progression and suppress the cyclin E-CDK2 activity, although the transcriptional activity of CDX2 may also make some contribution to the cell-proliferation block.

Correlation between CDX2 and $p27^{Kip1}$ levels in human colon cancer tissues

Finally, we analyzed expression of CDX2 and $p27^{Kip1}$ proteins in 59 human colon cancer specimens, and investigated possible correlation between their levels. Among these tumors, 28 showed the lower level of CDX2 protein compared with that in normal mucosa (Nl; Fig. 6A and 6D), whereas the other 31 showed CDX2 at similar to those at higher levels (Fig. 6B–D). Notably, the $p27^{Kip1}$ level was reduced in 21 of the 28 low-CDX2 tumors (75%; Fig. 6A and D; Supplementary Fig. S9), whereas it was reduced in only 10 of the 31 high-CDX2 tumors (Fig. 6B–D, 32%; $P < 0.001$, obtained from χ^2 test). These data are consistent with the results that the $p27^{Kip1}$ level was reduced in the low-CDX2 colon cancer cell lines and $Cdx2^{+/-}$ mutant mouse colonic tumors (Fig. 3D). Collectively, these results suggest that low levels of CDX2 contribute to the reduced levels of $p27^{Kip1}$ in human colon cancer tissues. On the contrary, $p27^{Kip1}$ protein in 21 of the 31 high-CDX2 tumors (68%; Fig. 6B–D; Supplementary Fig. S10), whereas it was retained in only 7 of the 28 low-CDX2 tumors (25%; Fig. 6D). These data are also consistent with the results that CDX2 increased the level of $p27^{Kip1}$ protein in colon cancer TetOff cells (Fig. 3C), showing a positive correlation between CDX2 and $p27^{Kip1}$ levels.

Discussion

In human cancer cells of the colon and other epithelial tissues, the level of $p27^{Kip1}$ is frequently reduced by its accelerated degradation through proteasomes (36, 37). The reduced level of $p27^{Kip1}$ is also correlated with poor prognosis, suggesting its tumor-suppressing activity (25). Consistently, homozygous $p27^{Kip1}$ mutation increased the number of intestinal polyps in *Apc* mutant mice by 5 to 6 times (38). In colon cancer cells, however, the mechanism that stimulates the degradation of $p27^{Kip1}$ was unknown. Here we have shown that homeobox transcription factor CDX2 stabilizes $p27^{Kip1}$ by blocking its proteolysis (Figs. 3 and 4). Interestingly, we have found a significant correlation between CDX2 and $p27^{Kip1}$ protein levels in human colon cancer tissues (Fig. 6). Our present results suggest that the decreased level of CDX2 is one of the causes that stimulate the $p27^{Kip1}$ proteolysis in colon cancer cells.

During the G1 to S transition, phosphorylation of $p27^{Kip1}$ at T187 triggers its proteasomal degradation through the SCF-SKP2 E3 ubiquitin ligase complex (24, 26–29). The levels of SKP2 and Cks1 were not affected by expression of CDX2:R237A that increased $p27^{Kip1}$ (Fig. 3C, left), suggesting that CDX2 stabilizes $p27^{Kip1}$ protein independent of SKP2 and Cks1 levels. Notably, the extent of $p27^{Kip1}$ phosphorylation at T187 decreased on expression of CDX2 (Fig. 4D), suggesting that CDX2 suppressed the SKP2-dependent proteolysis of $p27^{Kip1}$, which caused $p27^{Kip1}$ accumulation (Fig. 3C). Consistently, the level of $p27^{Kip1}$ ubiquitylation was reduced on expression of CDX2 (Fig. 4C). On the contrary, the reduced activity of cyclin

Published OnlineFirst on January 11, 2011; DOI:10.1158/0008-5472.CAN-10-2842

E-CDK2 can stabilize $p27^{Kip1}$ because cyclin E-CDK2 phosphorylates $p27^{Kip1}$ at T187 and accelerates its proteasomal degradation (24, 26–29). Importantly, reducing the level of $p27^{Kip1}$ blocked decreases in the cyclin E-CDK2 activity and S-phase fraction caused by CDX2 (Fig. 5C and Fig. 5D). These results indicate that $p27^{Kip1}$ is a critical downstream target of CDX2 in regulating the cyclin E-CDK2 activity and blocking cell-cycle progression. Thus, $p27^{Kip1}$ stabilization may precede the attenuated activity of cyclin E-CDK2 in CDX2-induced cells (Fig. 3A and C). It remains to be investigated how CDX2 reduces the level of $p27^{Kip1}$ phosphorylation at T187.

The level of $p27^{Kip1}$ phosphorylation at S10 was also decreased on expression of CDX2 (Fig. 4D). Because the S10 dephosphorylation promotes binding of $p27^{Kip1}$ to cyclin-CDK complex, it helps $p27^{Kip1}$ to inhibit the cyclin-CDK activity and suppress tumor development (30, 31). Thus, it is conceivable that the reduced $p27^{Kip1}$ phosphorylation at S10 also contributes to the tumor-suppressive function of CDX2.

Interestingly, knocking down $p27^{Kip1}$ completely blocked the decreases in the cyclin E-CDK2 activity and S-phase fraction on expression of the mutant C2HD-N1:R237H or C2HD-N1:R237A that lacked transcriptional activity and C-terminal domain of CDX2 (Fig. 5C and D; Supplementary Fig. S8). These results show that CDX2 stabilizes $p27^{Kip1}$ through the nontranscriptional function mediated by its N-terminal and homeobox domains. The results have also prompted us to question whether the transcription-independent function of CDX2 is shared among the CDX family proteins. To address this issue, we constructed DLD-1–TetOff cells that expressed CDX1 (Supplementary Fig. S11A), the closest homolog of CDX2. The CDXs show a high similarity in their HDs (aa identity, 92%; and similarity, 97%: Supplementary Fig. S12A), but only low similarities in both N-terminal and C-terminal domains (aa similarities, 42% and 38%, respectively: Supplementary Fig. S12B and C). Expression of CDX1 did not increase the $p27^{Kip1}$ level in the DLD-1 cells (Supplementary Fig. S11C), although the level of induced CDX1 and its transcriptional activity were comparable to those of CDX2 (Supplementary Fig. S11A and B). Thus, it appears that the transcription-independent block of proliferation is specific to CDX2. Because the HDs are almost identical between the CDXs (Supplementary Fig. S12A), the N-terminal domain can be critical for the nontranscriptional function of CDX2. This interpretation is consistent with the results that C2HD-N1 (N-terminal and HD) increases the level of $p27^{Kip1}$ protein by approximately 5 times, whereas C2HD-KK alone does it only by approximately 1.5 times (Fig. 3C, left; Supplementary Fig. S7A, center). To understand the precise role of the N-terminal domain of CDX2 in stabilizing $p27^{Kip1}$, it will be interesting to identify proteins that can bind to the domain.

Wnt, Notch, and PI3K-Akt signaling pathways are proposed as major mechanisms that stimulate proliferation of the colonic epithelial cells (16, 39, 40). On the contrary, the $Cdx2^{+/-}$ mutation stimulated proliferation of the $Apc^{-/-}$ adenoma epithelial cells in which Wnt and Notch signaling pathways were already activated (Fig. 1C; refs. 16, 39, 40). Expression of CDX2 also blocked the proliferation of colon cancer cells in which the Wnt and PI3K signaling pathways were activated through mutations in the *APC*, β-catenin, or *PIK3CA* gene (Fig. 1D; refs. 16, 17). Collectively, these results may indicate that CDX2 functions as an additional layer of regulation that inhibits proliferation of the colonic epithelial cells, and ensures a quick halt of the cell cycle as soon as the transit-amplifying cells initiate differentiation.

Disclosure of Potential Conflicts of Interest

No potential conflicts of interest disclosed.

Acknowledgments

We thank M. Maekawa for technical assistance and Dr. A. Shimizu for the flow cytometry service. We also thank Drs. G. Baldassarre, M. Schiappacassi, T. Yamashita, and M. Sonoshita for fruitful discussion, and Drs. K. Ookawa and M. Sugai for technical advice. We thank Dr. Y. Tamai for *Cdx2* mutant mice.

Grant Support

This work was supported by grants-in-aid for scientific research (to M. M. Taketo) and for young scientist B (to K. Aoki) from the Ministry of Education, Culture, Sports, Science, and Technology, Japan.

The costs of publication of this article were defrayed in part by the payment of page charges. This article must therefore be hereby marked *advertisement* in accordance with 18 U.S.C. Section 1734 solely to indicate this fact.

Received August 4, 2010; revised October 4, 2010; accepted October 4, 2010; published OnlineFirst January 11, 2011.

References

1. James R, Kazenwadel J. Homeobox gene expression in the intestinal epithelium of adult mice. J Biol Chem 1991;266:3246–51.
2. Macdonald PM, Struhl G. A molecular gradient in early Drosophila embryos and its role in specifying the body pattern. Nature 1986;324:537–45.
3. Niwa H, Toyooka Y, Shimosato D, Strumpf D, Takahashi K, Yagi R, et al. Interaction between Oct3/4 and Cdx2 determines trophectoderm differentiation. Cell 2005;123:917–29.
4. Chawengsaksophak K, James R, Hammond VE, Kontgen F, Beck F. Homeosis and intestinal tumours in *Cdx2* mutant mice. Nature 1997;386:84–7.
5. Tamai Y, Nakajima R, Ishikawa T, Takaku K, Seldin MF, Taketo MM. Colonic hamartoma development by anomalous duplication in *Cdx2* knockout mice. Cancer Res 1999;59: 2965–70.
6. Silberg DG, Swain GP, Suh ER, Traber PG. Cdx1 and cdx2 expression during intestinal development. Gastroenterology 2000;119:61–971.
7. Guo RJ, Suh ER, Lynch JP. The role of Cdx proteins in intestinal development and cancer. Cancer Biol Ther 2004;3:593–601.
8. Gao N, Kaestner KH. Cdx2 regulates endo-lysosomal function and epithelial cell polarity. Genes Dev 2010;24:1295–305.
9. Gao N, White P, Kaestner KH. Establishment of intestinal identity and epithelial-mesenchymal signaling by Cdx2. Dev Cell 2009;16:588–99.
10. Ee HC, Erler T, Bhathal PS, Young G. P, James R. J. Cdx-2 homeodomain protein expression in human and rat colorectal adenoma and carcinoma. Am J Pathol 1995;147:586–92.
11. Mallo GV, Rechreche H, Frigerio JM, Rocha D, Zweibaum A, Lacasa M, et al. Molecular cloning, sequencing and expression of the mRNA encoding human *Cdx1* and *Cdx2* homeobox. Down-regulation of

Published OnlineFirst on January 11, 2011; DOI:10.1158/0008-5472.CAN-10-2842

Cdx1 and *Cdx2* mRNA expression during colorectal carcinogenesis. Int J Cancer 1997;74:35–44.

12. Aoki K, Tamai Y, Horiike S, Oshima M, Taketo MM. Colonic polyposis caused by mTOR-mediated chromosomal instability in $Apc^{+/\Delta 716}Cdx2+/-$ compound mutant mice. Nat Genet 2003;35: 323–30.
13. Oshima M, Oshima H, Kitagawa K, Kobayashi M, Itakura C, Taketo M. Loss of *Apc* heterozygosity and abnormal tissue building in nascent intestinal polyps in mice carrying a truncated *Apc* gene. Proc Natl Acad Sci U S A 1995;92:4482–6.
14. Bonhomme C, Duluc I, Martin E, Chawengsaksophak K, Chenard MP, Kedinger M, et al. The *Cdx2* homeobox gene has a tumour suppressor function in the distal colon in addition to a homeotic role during gut development. Gut 2003;52:1465–71.
15. Kakizaki F, Aoki K, Miyoshi H, Carrasco N, Aoki M, Taketo MM. CDX transcription factors positively regulate expression of solute carrier family 5, member 8 in the colonic epithelium. Gastroenterology 2010;138:627–35.
16. van de Wetering M, Sancho E, Verweij C, de Lau W, Oving I, Hurlstone A, et al. The β-catenin/TCF-4 complex imposes a crypt progenitor phenotype on colorectal cancer cells. Cell 2002;111:241–50.
17. Samuels Y, Diaz LA Jr, Schmidt-Kittler O, Cummins JM, Delong L, Cheong I, et al . Mutant PIK3CA promotes cell growth and invasion of human cancer cells. Cancer Cell 2005;7:561–73.
18. Hinoi T, Lucas PC, Kuick R, Hanash S, Cho KR, Fearon ER, CDX2 regulates liver intestine-cadherin expression in normal and malignant colon epithelium and intestinal metaplasia. Gastroenterology 2002; 123:1565–77.
19. Hinoi T, Gesina G, Akyol A, Kuick R, Hanash S, Giordano TJ, et al . CDX2-regulated expression of iron transport protein hephaestin in intestinal and colonic epithelium. Gastroenterology 2005;128:946–61.
20. Gehring WJ, Qian YQ, Billeter M, Furukubo-Tokunaga K, Schier AF, Resendez-Perez D, et al. Homeodomain-DNA recognition. Cell 1994;78:211–23.
21. Chi, Y. I. Homeodomain revisited: a lesson from disease-causing mutations. Hum Genet 2005;116: 433-444.
22. Rings EH, Boudreau F, Taylor JK, Moffett J, Suh ER, Traber PG. Phosphorylation of the serine 60 residue within the Cdx2 activation domain mediates its transactivation capacity. Gastroenterology 2001;121:1437–50.
23. Sherr CJ, Roberts JM. CDK inhibitors: positive and negative regulators of G1-phase progression. Genes Dev 1999;13:1501–12.
24. Vlach J, Hennecke S, Amati B. Phosphorylation-dependent degradation of the cyclin-dependent kinase inhibitor p27. EMBO J 1997; 16:5334–44.
25. Chu IM, Hengst L, Slingerland JM. The Cdk inhibitor p27 in human cancer: prognostic potential and relevance to anticancer therapy. Nat Rev Cancer 2008;8:253–67.
26. Montagnoli A, Fiore F, Eytan E, Carrano AC, Draetta GF, Hershko A, et al. Ubiquitination of p27 is regulated by Cdk-dependent phosphorylation and trimeric complex formation. Genes Dev 1999;13: 1181–9.
27. Carrano AC, Eytan E, Hershko A, Pagano M. SKP2 is required for ubiquitin-mediated degradation of the CDK inhibitor p27. Nat Cell Biol 1999;1:193–9.
28. Nakayama KI, Hatakeyama S, Nakayama K. Regulation of the cell cycle at the G1-S transition by proteolysis of cyclin E and $p27^{Kip1}$. Biochem Biophys Res Commun 2001;282:853–60.
29. Sutterluty H, Chatelain E, Marti A, Wirbelauer C, Senften M, Muller U, et al. $p45^{SKP2}$ promotes $p27^{Kip1}$ degradation and induces S phase in quiescent cells. Nat Cell Biol 1999;1:207–14.
30. Kotake Y, Nakayama K, Ishida N, Nakayama KI. Role of serine 10 phosphorylation in p27 stabilization revealed by analysis of p27 knock-in mice harboring a serine 10 mutation. J Biol Chem 2005;280: 1095–102.
31. Besson A, Gurian-West M, Chen X, Kelly-Spratt KS, Kemp CJ, Roberts JM. A pathway in quiescent cells that controls $p27^{Kip1}$ stability, subcellular localization, and tumor suppression. Genes Dev 2006;20:47–64.
32. Kossatz U, Vervoorts J, Nickeleit I, Sundberg HA, Arthur JS, Manns MP, et al. C-terminal phosphorylation controls the stability and function of $p27^{kip1}$. EMBO J 2006;25:5159–70.
33. Liang J, Shao SH, Xu ZX, Hennessy B, Ding Z, Larrea M, et al. The energy sensing LKB1-AMPK pathway regulates p27(kip1) phosphorylation mediating the decision to enter autophagy or apoptosis. Nat Cell Biol 2007;9:218–24.
34. Berthet C, Klarmann KD, Hilton MB, Suh HC, Keller JR, Kiyokawa H, et al. Combined loss of Cdk2 and Cdk4 results in embryonic lethality and Rb hypophosphorylation. Dev Cell 2006;10:563–73.
35. Hinds PW, Mittnacht S, Dulic V, Arnold A, Reed SI, Weinberg RA. Regulation of retinoblastoma protein functions by ectopic expression of human cyclins. Cell 1992;70:993–1006.
36. Chu I, Sun J, Arnaout A, Kahn H, Hanna W, Narod S, et al. p27 phosphorylation by Src regulates inhibition of cyclin E-Cdk2. Cell 2007;128:281–94.
37. Loda M, Cukor B, Tam SW, Lavin P, Fiorentino M, Draetta GF, et al. Increased proteasome-dependent degradation of the cyclin-dependent kinase inhibitor p27 in aggressive colorectal carcinomas. Nat Med 1997;3:231–4.
38. Philipp-Staheli J, Kim KH, Payne SR, Gurley KE, Liggitt D, Longton G, et al. Pathway-specific tumor suppression. Reduction of p27 accelerates gastrointestinal tumorigenesis in *Apc* mutant mice, but not in *Smad3* mutant mice. Cancer Cell 2002;1:355–68.
39. He X C, Yin T, Grindley JC, Tian Q, Sato T, Tao WA, et al. PTEN-deficient intestinal stem cells initiate intestinal polyposis. Nat Genet 2007;39:189–98.
40. van Es J H, Jay P, Gregorieff A, van Gijn ME, Jonkheer S, Hatzis P, et al. Wnt signalling induces maturation of Paneth cells in intestinal crypts. Nat Cell Biol 2005;7:381–6.
41. Gu Y, Rosenblatt J, Morgan DO. Cell cycle regulation of CDK2 activity by phosphorylation of Thr160 and Tyr15. EMBO J 1992;11:3995–4005.
42. Ishida N, Kitagawa M, Hatakeyama S, Nakayama K. Phosphorylation at serine 10, a major phosphorylation site of p27(Kip1), increases its protein stability. J Biol Chem 2000;275:25146–54.

Exp. Anim. 59(2), 147–155, 2010

—Original—

Genetic Analyses of Fancy Rat-Derived Mutations

Takashi KURAMOTO, Mayuko YOKOE, Kayoko YAGASAKI, Tatsuya KAWAGUCHI, Kenta KUMAFUJI, and Tadao SERIKAWA

Institute of Laboratory Animals, Graduate School of Medicine, Kyoto University, Yoshidakonoe-cho, Sakyo-ku, Kyoto 606-8501, Japan

Abstract: To collect rat mutations and increase the value of the rat model system, we introduced fancy-derived mutations to the laboratory and carried out genetic analyses. Six fancy rats were shipped from a fancy rat colony in the USA and used as founders. After initial crosses with a laboratory strain, TM/Kyo or PVG/Seac, inbreeding started and 6 partially inbred lines, including 2 sublines, were produced as Kyoto Fancy Rat Stock (KFRS) strains. During inbreeding, we isolated 9 mutations: 5 coat colors, American mink (*am*), Black eye (*Be*), grey (*g*), Pearl (*Pel*), siamese (*sia*); 1 coat pattern, head spot (*hs*); 2 coat textures, Rex (*Re*), satin (*sat*); and an ear pinnae malformation, dumbo (*dmbo*). Genetic analyses mapped 7 mutations to particular regions of the rat chromosomes (Chr): *am* to Chr 1, *sia* to Chr 1, *sat* to Chr 3, *Re* to Chr 7, *g* to Chr 8, *dmbo* to Chr 14, and *hs* to Chr 15. Candidate gene analysis revealed that a missense mutation in the tyrosinase gene, Ser79Pro, was responsible for *sia*. From mutant phenotypes and mapping positions, it is likely that all mutations isolated in this study were unique to the fancy rat. These findings suggest that fancy rat colonies are a good source for collecting rat mutations. The fancy-derived mutations, made available to biomedical research in the current study, will increase the scientific value of laboratory rats.
Key words: bioresource, coat color, genetic mapping, inbreeding, mutation

Introduction

Genetic analyses of common diseases in humans have revealed that gene mutations are involved in diseases. Genome sequencing projects of various mammalian species followed by comparative genome analyses have revealed that a large number of genes are shared among species. Thus, it is thought that mutations found in model animals and animals carrying such mutations can contribute to the better understanding of human diseases.

The laboratory rat (*Rattus norvegicus*) has been widely used as an animal model of human diseases, because its size is suitable for manipulation [1, 27]. Sequencing of the rat genome has shown that the rat has about 20,000 predicted genes and shares as many as 90% with humans [9]. So far, at least 70 mutations have been identified as causative genes of specific diseases and rat strains carrying such mutations can be used as good animal models for these diseases; however, considering the high number of rat genes predicted [9], more mutations will be required to investigate the full range of diseases. Thus,

(Received 25 August 2009 / Accepted 22 October 2009)
Address corresponding: T. Kuramoto, Institute of Laboratory Animals, Graduate School of Medicine, Kyoto University, Yoshidakonoe-cho, Sakyo-ku, Kyoto 606-8501, Japan

collecting rat mutations and making rats carrying these mutations available as bioresources would enhance the scientific value of rats as an animal model for human diseases.

There are several approaches to collecting rat mutations. They include discovering naturally occurring mutations and inducing mutations by random mutagenesis [21]. In addition, attempts have been made to collect mutations outside of the laboratory, from the field or fancy rat colonies; indeed, some inbred strains have been established from wild captured rats [11]. However, fancy rats have not been surveyed as a source of mutations, with a few exceptions [26].

Fancy rat colonies have potential as a source for collecting novel rat mutations, because various mutations are considered to persist only in fancy rats, largely coat and eye color mutations, and coat pattern mutations. Thus, when they are available in laboratory rats, most will provide opportunities to study the function of melanocytes, which are not only responsible for pigment synthesis in the skin and hair, but are also involved in inner ear and eye functions [30]. In addition, in human, dysfunctions of melanocytes result in skin disorders such as oculocutaneous albinism, piebaldism and skin cancers [12, 29], prompting us to introduce mutations found in the current fancy rat colonies to the laboratory and establish them as novel bioresources available for biomedical research.

In this study, we imported 6 fancy rats from a fancy rat colony in the USA to our laboratory. We tried to isolate fancy mutations and establish inbred strains carrying them. During inbreeding, we isolated 9 mutations, of which 7 were mapped to particular genomic regions of rat chromosomes. A coat color mutation, siamese, was identified as a missense mutation in the rat tyrosinase gene.

Materials and Methods

Animals

In July, 2005, 6 fancy rats were imported from a fancy rat colony named Spoiled Ratten Rattery (SRR) kept by Ms. E. Brooks in Kansas City, Missouri, USA (http://www.spoiledratten.com/index.html). These rats (SRR01-06) were used as founders to establish fancy-derived strains. SRR01 was female and the others were males. It was known that these founders carried the following mutations (Table 1): SRR01 carried dumbo (*dmbo*), Rex (*Re*), and satin (*sat*); SRR02 carried *sat* and siamese (*sia*); SRR03 carried American mink (*am*), grey (*g*), and Pearl (*Pel*); SRR04 carried dumbo (*dmbo*); SRR05 carried *Re*; and SRR06 carried Black eye (*Be*). TM/Kyo and PVG/Seac rats were selected as mating partners to obtain progeny from the founder fancy rats, because they are homozygous for nonagouti (*a/a*) and hooded (*h/h*) recessive mutations. SRR01, SRR05, and SRR06 were crossed with the TM/Kyo strain and SRR02, SRR03, and SRR04 were crossed with the PVG/Seac strain. Following caesarean operations, F_1 hybrids were introduced to specific pathogen-free (SPF) facilities in our institute. Brother-sister mating was carried out to establish fancy rat-derived strains for each founder. At each generation during inbreeding, rats showing the mutant phenotypes were selected. When different mutant phenotypes were found in an inbreeding line, sublines were separated.

To map the mutations isolated from fancy rats, a male rat representing each strain was used to make F_1 hybrids with BN/SsNSlc (BN) or WTC/Kyo (WTC) female rats.

Animal care and experimental procedures were approved by the Animal Research Committee, Kyoto University and were conducted according to the Regulation on Animal Experimentation at Kyoto University.

Genetic mapping

To map *sat* and *sia* mutations, SRR02 (F5) was mated with BN rats and 82 backcross progeny (BCP) were produced (cross 1). To map *am*, SRR03-*am* (F6) was mated with BN rats and 98 BCP were produced (cross 2). To map *g* and *Pel*, SRR03-*g*, *Pel* (F6) was mated with BN rats and 87 BCP were produced (cross 3). To map *dmbo* and *hs*, SRR04 (F5) was mated with BN rats and 99 BCP were produced (cross 4). To map *Re*, SRR05 (F3) was mated with BN rats and 50 BCP were produced (cross 5). To map *Be*, SRR06 (F6) was mated with BN and WTC rats, and 48 and 67 BCP were produced (crosses 6 and 7).

Genotyping was performed as described previously [16] with a set of highly informative simple sequence length polymorphism (SSLP) markers [20].

Table 1. Mutations isolated from fancy rats

Mutation (symbol)	MP term (MP id)[a]	Characteristic	Origin[b]	KFRS strain	Mode of inheritance	Mapped position in rats		Candidate gene name (Gene symbol)	Mutant phenotype of candidate gene in mice
						Chr	Physical position[c]		
American mink (*am*)	diluted coat color (0000371)	Light brown body hair [26]	Unknown. Different from the original mink described by Robinson	KFRS3A/ Kyo	recessive	1	95.5–103 Mb[d]	Hermansky-Pudlak syndrom 5 (*Hps5*)	Mice Homozygous for *Hps5* mutation (*ruby-2*) have hypopigmented eyes and hair [33]
Black eye (*Be*)	diluted coat color (0000371)	Cream coat with pigmented eyes	Laboratory colony at Edinburgh University in Scotland in 1998 → Breeder in England	KFRS6/ Kyo	dominant	ND	ND		
dumbo (*dmbo*)	abnormal outer ear morphology (0002177)	Ears are set lower on the head, and are larger and rounder.	Fancy rats somewhere in the northwest US	KFRS4/ Kyo	recessive	14	79.0–84.7 Mb	H6 homeo box 1 (*Hmx1*)	Mice carrying *Hmx1* mutations exhibit enlarged ear pinnae with a distinctive ventrolateral shift [23]
grey (*g*)	diluted coat color (0000371)	Light grey body hair	Maybe Russian blue. From fancies of east coast US.	KFRS3B/ Kyo	recessive	8	57.3–95.2 Mb	RB27A, member RAS oncogene family (*Rab27a*) myosin VA (*Myo5a*)	Gene defects produce abnormal pigmentation and a gray or diluted coat color in ashen or dilute mice [22, 32] and dop rats [8].
head spot (*hs*)	head head spot (0002939)	White spotting on the head	Unknown	KFRS4/ Kyo	recessive	15	84.6–91.2 Mb	endothelin receptor type B (*Ednrb*)	Mice homozygous for the *Ednrbs* mutation show irregular white spotting, depending on the genetic background [25]
Pearle (*Pel*)	diluted coat color (0000371), embryonic lethality (0008762)	Lighter coat color expressed on mink or grey. Homozygotes die in the embryonic period (E10–E12)	English fancy [26]	KFRS3A/ Kyo KFRS3B/ Kyo	dominant	ND	ND		
Rex (*Re*)	wavy hair (0000410), nude (0003815), wavy vibrissae (0001279)	Heterozygotes show wavy body hair, while homozygotes lose body hair after the first molt. Both heterozygotes and homozygotes show wavy vibrissae.	England → Breeder in California	KFRS5/ Kyo	dominant	7	135–143 Mb[d]	keratin 71 (*Krt71*)	Mouse mutations in the *Krt71* gene. caracul (*Ca*), cause wavy coat hairs in *Ca/+* heterozygous mice [14]
satin (*sat*)	abnormal coat appearance (0001510), curly vibrissae (0001274)	Longer hair and shiny-looking "greasy" hair. Vibrissae are bent downward.	Fancy rats kept by a breeder in California	KFRS2/ Kyo	recessive	3	105.8–114.9 Mb	fibroblast growth factor 7 (*Fgf7*)	Mice lacking the *Fgf7* gene develop a matted coat [10]
siamese (*sia*)	diluted coat color (0000371)	Homozygotes show light body hair, but their ears, nose, tail, and scrotum are dark, as in Siamese cats. Eyes are slightly pigmented and appear red.	Laboratory in France in the 1980s → Breeder in UK → breeders in California	KFRS2/ Kyo	recessive	1	140.6–145.5 Mb	tyrosinase (*Tyr*)	Mice homozygous for Tyr^{c-h} show light coat color and darkened ears, nose, and scrotum. [18]

[a]: Mutant phenotypes are classified by mammalian phenotype ontology. [b]: Provided by Ms. E. Brooks. [c]: RGSC v3.4. [d]: Expected theoretical maximum distance between *am* or *Re* and non-recombinant markers. Physical distance corresponding to 1 cM was expected to be 1 Mb.

Direct sequencing of the Tyr gene of Black-eyed and Siamese rats

Direct sequencing was performed as described previously [17]. Rat *Tyr* exons were amplified with the following 6 sets of primers: rTyr-1&2 (exon 1,463 bp), 5'-TGTTTGAGCAGATCTTGTACGG-3' and 5'-TGTTTTGCCAAAGTGAGGTAA-3'; rTyr-3&11 (exon 1,633 bp) 5'-GCGGAAACTGTAAGTTTGGA-3' and 5'-AAGGTTCCTTTTCTGTGCTGA-3'; rTyr-12&13 (exon 2,398 bp), 5'-TTTCATTCATATGTAAGTCCCTTG-3' and 5'-GCTTAGCATTGCAAAACTCACA-3'; rTyr-14&15 (exon 3,384 bp), 5'-TTGTTTATTTAAAATTAGGCTTACCTC-3' and 5'-TCTCAAAATAGAGAACCACCACAA-3'; rTyr-16&17 (exon 4,488 bp), 5'-AAAGTTTGAAGATAGTCAGCATTTGA-3' and 5'-TTTAGCTGTACAAAATATCCTTGAAA-3'; rTyr-18&10 (exon 5,489 bp), 5'-GCACTCAAACCCAAGCATCT-3' and 5'-TTCCTTAGAAACTGGGACGTG-3'.

Examination of fetuses at cesarean section

Six wild-type SRR03 females (+/+) and six *Pel*-heterozygous female SRR03 (*Pel*/+) rats were mated with the *Pel*-heterozygous SRR03 males (*Pel*/+). At P20, fetuses were removed by cesarean section. The numbers of corpora lutea, live fetuses, and embryo-fetal deaths were counted. Embryo-fetal deaths were categorized into early death (implantation sites, resorbed embryos, and placental remnants) and late death (early macerated fetuses, late macerated fetuses, and dead fetuses). The number of implantations was calculated from the sum of the number of live fetuses and the number of embryo-fetal deaths.

Statistical analysis

To determine the mode of inheritance and linkage relationship, chi-square tests were performed. When the *P* value of chi-square for 1:1 was more than 0.05, the mutation was thought to be an autosomal single gene. When the *P* value of chi-square for linkage was less than 0.05, the linkage relationship between loci was thought to be significant. For statistical analysis of embryo-fetal deaths found in the Pearl mutant, Student's *t*-test was performed using Microsoft Excel.

Results

Fancy rat-derived strains

We isolated 9 mutations during inbreeding and assigned "Mammalian Phenotype terms (MP)" to their mutant phenotypes to make it easy to understand them [31] (Table 1). They involved 5 coat color mutations (*am*, *Be*, *g*, *Pel*, and *sia*), 1 coat pattern mutation (*hs*), 2 coat texture mutaions (*Re* and *sat*), and an ear pinnae malformation mutation (*dmbo*). The Pearl phenotype manifested in conjunction with homozygous status for *am* or *g*.

During inbreeding, the line originating from SRR01 became extinct. Although inbreeding was not fully completed, we tentatively named the derived lines Kyoto Fancy Rat Stock (KFRS). Each strain was defined with a number representing the names of the founder rats, and sublines were defined by the addition of a letter after the number. Six lines, including sublines, were produced and their strain names, mutations they carried, and generations at the end of February, 2010 were as follows: KFRS2/Kyo carrying *sat* and *sia* (F18), KFRS3A/Kyo carrying *am* and *Pel* (F19), KFRS3B/Kyo carrying *g* and *Pel* (F20), KFRS4/Kyo carrying *dmbo* and *hs* (F18), KFRS5A/Kyo carrying *Re* (F19), and KFRS6/Kyo carrying *Be* (F17) (Fig. 1 and Table 1).

Mode of inheritance and genetically mapped region of fancy mutations

In cross 1, 40 had satin-type body hair and 42 had normal body hair. Thirty-six had a siamese coat color, while forty-six had normal coat color. These findings indicated that both the *sat* and *sia* mutations were autosomal recessive. The linkage map including *sat* was *D3Got76* – 1.2 cM – *D3Got69*, *sat* – 1.2 cM – *D3Mco2*. The *sat* locus spanned the 9.1-Mb region defined by *D3Got76* and *D3Mco2*. The linkage map including *sia* was *D1Rat273* – 2.4 cM – *sia* – 2.4 cM – *D1Rat138*. The *sia* locus spanned the 4.9-Mb region defined by *D1Rat273* and *D1Rat138*.

In cross 2, 47 had American mink-type body hair and 51 had normal body hair, indicating the *am* mutation was autosomal recessive. The *am* showed no recombination with *D1Rat214* and *D1Mgh35* in 98 meioses, which indicated that *am* was located <3.0 cM away from these

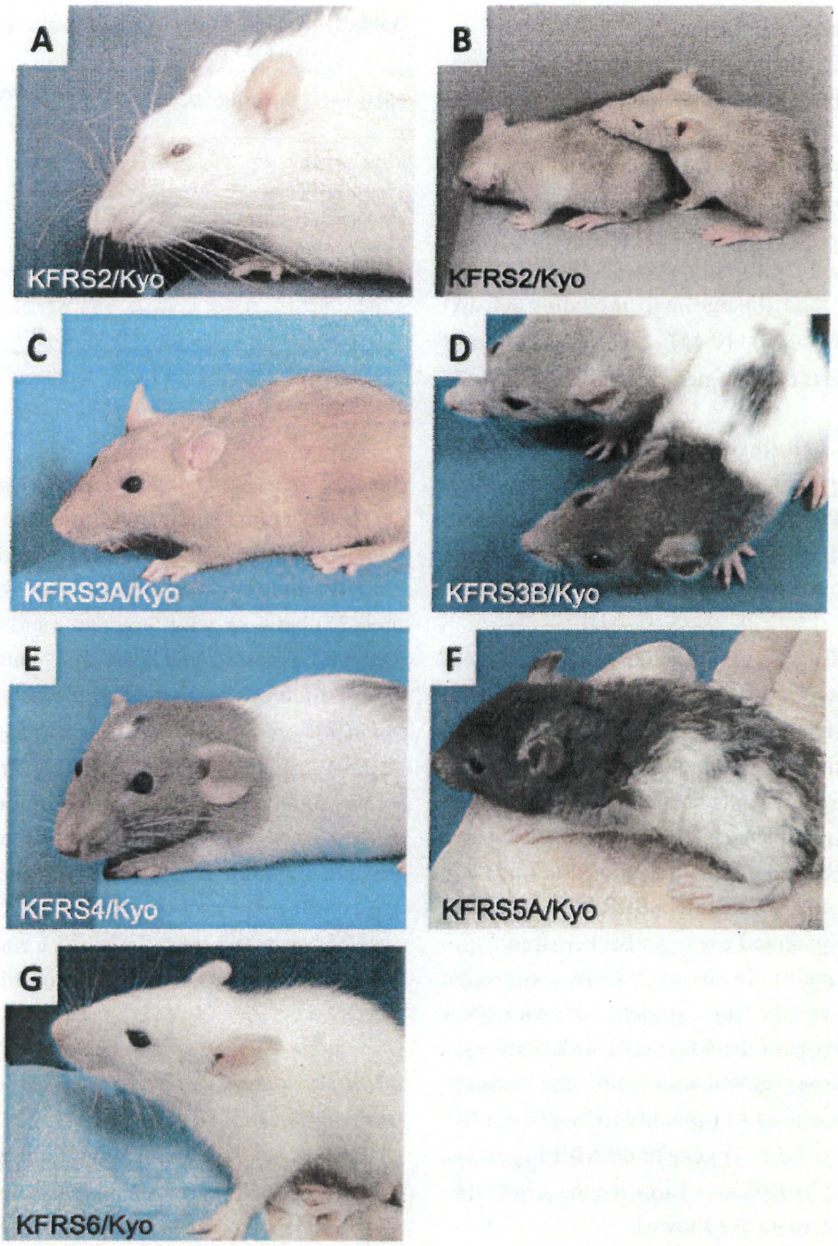

Fig. 1. Kyoto Fancy Rat Stock (KRFS) strains. (A) KFRS2/Kyo, 2 months of age, *sat/sat*, *sia/sia*. (B) KFRS2/Kyo, 3 weeks of age, Left; *sat/+*, *sia/sia*. Right; *sat/sat*, *sia/sia*. Note that siamese marking of the nose is apparent in the adult *sia/sia* rat, compared with the young rat. (C) KFRS3A/Kyo, *am/am*. (D) KFRS3B/Kyo, Upper; *g/g*, *Pel/+*. Lower; *g/g*. (E) KFRS4/Kyo, *dmbo/dmbo*, *hs/hs*. (F) KFRS5/Kyo, *Re/+*. (G) KFRS6/Kyo, *Be/Be*, *c/c*. All strains are homozygous for *a*.

markers with 95% probability [7].

In cross 3, 46 had grey-type body hair and 41 had normal body hair, indicating the *g* mutation was autosomal recessive. The linkage map including *g* was *D8Rat36* – 6.9 cM – *D8Rat182*, *g* – 14.9 cM – *D8Rat131*. The *g* locus spanned the 37.9-Mb region defined by

D8Rat36 and *D8Rat131*.

In cross 4, 55 had dumbo-type ears and 44 had normal ears. Forty-five had white spots on their head and fifty-four had no head spots. These findings indicated that both *dmbo* and *hs* mutations were autosomal recessive. The linkage map including *dmbo* was *D14Arb10* – 1.0 cM – *D14Rat37*, *dmbo* – 6.1 cM – *D14Rat57*. The *dmbo* locus spanned the 5.7-Mb region defined by *D14Rat10* and *D14Rat57*. The linkage map including *hs* was *D15Got78* – 5 cM – *hs* – 12 cM – *D15Rat26*. The *hs* locus spanned the 6.6-Mb region defined by *D15Got78* and *D15Rat26*.

In cross 5, 24 had Rex-type body hair and 26 had normal body hair, indicating that the *Re* mutation was autosomal dominant. *Re* showed no recombination with *D7Mit1* and *D7Rat80* in 50 meioses, indicating that *Re* was located <5.8 cM from these markers with 95% probability [7].

Using crosses 6 and 7, we carried out genetic analysis of the *Be* mutation. In rat fanciers, it is known that the *Be* mutation masks the coat color only in combination with the albino mutation. This combination produces rats with a pale creamy white coat color and black eyes. To elucidate the inheritance pattern of the black eye, we first crossed a SRR06 male with BN/SsNSlc (*a/a*, *b/b*, *C/C*) rats. Since all (BN/SsNSlc × SRR06)F_1 rats had a black coat and pigmented eyes, we backcrossed F_1 females to SRR06 males. In cross 6, 27 had a white coat with black eyes, and 21 had a colored coat with black eyes. The phenotype of the white coat with black eyes was completely cosegregated with a missense mutation at *Tyr*, Arg299His, found in the albino Wistar rat [4]. Direct sequencing of the *Tyr* gene of the SRR06 genome demonstrated that SRR06 also harbored the Arg299His missense mutation (data not shown).

To elucidate the inheritance pattern of the black eye on the *albino* background, we crossed a SRR06 male with albino WTC/Kyo (*a/a*, *B/B*, *c/c*) rats. All (WTC/Kyo × SRR06)F_1 rats had a white coat and black eyes. We then backcrossed the F_1 females to WTC/Kyo males. In cross 7, 29 had a white coat with black eyes, and 38 had a colored coat with black eyes. These findings indicated that the *Be* mutation was a single autosomal mutation and manifested dominantly only in the presence of the albino mutation in the homozygous state.

Table 2. Number of embryo-fetal deaths found in Pearl mutants

Stage of embryo-fetal death	Cross to produce embryos	
	+/+ × Pel/+	*Pel/+ × Pel/+*
Implantation site	0.0 ± 0.0	0.0 ± 0.0
Resorbed embryo	0.2 ± 0.4	3.0 ± 0.6**
Placental remnant	0.0 ± 0.0	0.5 ± 0.5*
Early macerated fetus	0.0 ± 0.0	0.0 ± 0.0
Late macerated fetus	0.0 ± 0.0	0.0 ± 0.0
Dead fetus	0.0 ± 0.0	0.0 ± 0.0
Total	0.2 ± 0.4	3.5 ± 0.8**

*: $P<0.05$, **: $P<0.01$.

Embryonic lethality of the Pearl (Pel) mutation

There were no significant differences in the numbers of corpora lutea [12.5 ± 1.6 vs. 12.7 ± 0.8 (mean ± SD), P=0.42] and implantations (12.2 ± 1.6 vs. 11.7 ± 0.5, P=0.25) between wild-type (+/+) and Pearl (*Pel/+*) females both crossed with Pearl (*Pel/+*) males. Meanwhile, embryo-fetus deaths were significantly higher in (*Pel/+* × *Pel/+*)F_1 embryos than in (+/+ × *Pel/+*)F_1 embryos: 3.5 ± 0.8 vs. 0.2 ± 0.4, $P<0.01$ (Table 2). Embryo-fetus deaths found in (*Pel/+* × *Pel/+*)F_1 embryos included resorbed embryos (3.0 ± 0.6) and placental remnant (0.5 ± 0.5). The proportion of embryo-fetus deaths with regard to the number of corpora lutea in (*Pel/+* × *Pel/+*)F_1 was 27.5%, which agreed with 25% embryo-fetus death when homozygous lethality occurred in *Pel/Pel* embryos.

Identification of siamese as a missense mutation in the Tyrosinase gene

Tyrosinase (*Tyr*) was thought to be a good candidate for *sia*, because mouse *himalayan* mutation (*h*) at the *Tyr* locus showed an extremely similar coat color phenotype to the siamese rat. Direct sequencing revealed a missense mutation (c. 235 T>C, p. Ser79Pro) in exon 1 of the *tyrosinase* gene in the *sia/sia* homozygous genome (Fig. 2). This missense mutation was completely cosegragated with the siamese coat phenotype in 82 (BN × SRR02)F_1 × SRR02 BCP and was not found among 34 rat inbred strains (data not shown).

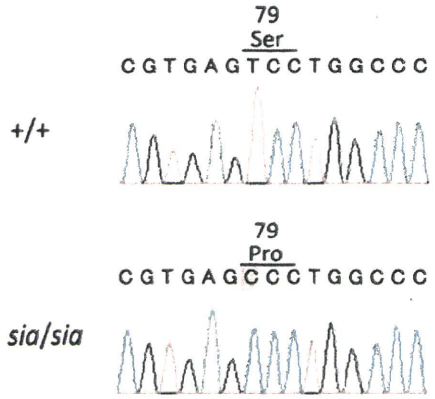

Fig. 2. Identification of siamese mutation. Sequence analysis of *Tyr* cDNA from wild-type and *sia/sia* rats. In the *sia/sia* rat, a nucleotide conversion T to C (red) was found at the position of nucleotide 253 of rat *Tyr* cDNA. The *sia* mutation converts the amino acid residue at codon 79 from serine (Ser) to proline (Pro).

Discussion

From mapped positions and phenotype resemblances to existing mutations of rats or mice, we selected candidate genes for the fancy mutations (Table 1). For *Myo5a* and *Ednrb*, rat mutations have been identified: dilute-opisthotonus (*dop*) mutation in *Myo5a* [8] and spotting lethal (*sl*) mutation in *Ednrb* [15]. We confirmed the absence of these mutations in *grey*-homozygous KFRS3B/Kyo and *head spot*-homozygous KFRS4/Kyo rats (data not shown). Therefore, all the fancy mutations isolated were likely to be unique and our study has made them available to the laboratory.

The Ser79Pro missense mutation was completely cosegregated with the siamese phenotype and was specific to KFRS2/Kyo. Missense mutations around the 79th amino acid of TYR provoke albinism in mice and humans, suggesting that this region plays an important role in hair and skin pigmentation [3, 24]. Therefore, we concluded that the S79P missense mutation is responsible for the siamese phenotype in rats. Tyrosinase is the key enzyme involved in the melanin biosynthetic pathway and is responsible for the rate limiting step [5]. Mutations in the *TYR* gene cause human oculocutaneous albinism 1 (OCA1) [24]. Although there are more than 100 mutations in the mouse *Tyr* locus, such as albino (Arg77Leu), himalayan (His420Arg), and chinchilla (Ala482Thr) [3], increasing the range of *Tyr* mutations will provide a wealth of information on the biology of tyrosinase and lead to better understanding of the pathogenesis of OCA1.

In addition to previous work on the Pearl phenotype [26], we revealed that approx. 25% embryos were largely resorbed, suggesting that *Pel/Pel* embryos die in the early stage of organogenesis (gestation days 10 to 12) [6]. There is a close relationship between *Pel* and agouti (*A*) [26]. In the current study, we carried out preliminary genetic analysis using 46 *g*-homozygous rats from cross 3. However, we failed to find a linkage relationship between *Pel* and *D3Mit2*, a SSLP marker located 2 cM apart from *A*, which suggests that multiple genetic determinants might be involved in the expression of *Pel*.

To our knowledge, this study is the first report on the systemic introduction of fancy-derived mutations to the laboratory. Fancy rats are considered to be a good source for developing a new bioresource of rats. They allow us to isolate rat mutations effectively. Usually, the rate at which new mutations arise spontaneously is exceedingly low: it is known that, on average, only one gamete in 100,000 is likely to carry a detectable mutation at any single locus naturally occurring mutation rate [28], which means that the discovery of mutations depends on chance. In this study, we could isolate 9 unique mutations from only 6 founder rats, and it took only a few generations to isolate them. Moreover, fancy rats are usually kept by outbreeding, so when they are subjected to inbreeding in the laboratory, hidden mutations sometimes manifest. Actually, we observed the cataract and sterile phenotypes, which were unknown in the SRR, at several generations after starting inbreeding (data not shown).

Fancy rat colonies are thought to be maintained relatively independent of laboratory rats and have unique breeding histories different from the laboratory rats [2]. Therefore, it is expected that the fancy-derived KFRS strains will retain their unique genetic background different from laboratory rats, although almost half of them are derived from laboratory rats. The IS/Kyo strain originates from a cross of a wild captured male rat with Wistar female rats [13] and shows a clearly different

genetic background from other strains [20]. Systematic phenotypic analysis of IS/Kyo rats uncovered their unique traits, such as hypotension and high body temperature, which implies that a wild-derived genome might confer these unique traits [19]. Following several generations, all KFRS strains will be established as full inbred strains. Thus, we consider that the systematic genotype and phenotype analyses of these KFRSs will reveal their genetic background and untapped unique traits, which make them potential disease models. Finally, phenotypically annotated KFRSs will contribute to increase the scientific value of rats.

Acknowledgments

The authors are grateful to E. Brooks for providing fancy rats, and Y. Asano and K. Katsumata for evaluating embryo-fetal deaths. KFRS2/Kyo, KFRS3A/Kyo, KFRS3B/Kyo, KFRS4/Kyo, KFRS5A/Kyo, and KFRS6/Kyo (NBRP Rat No. 0560, 0570, 0571, 0572, 0573, and 0574) are deposited in the National BioResource Project-Rat in Japan and are available from the Project (http://www.anim.med.kyoto-u.ac.jp/nbr). This work was supported in part by a Grant-in-aid for Cancer Research from the Ministry of Health, Labour and Welfare and Grants-in-aid for Scientific Research from the Japan Society for the Promotion of Science (21300153 to TK).

References

1. Aitman, T.J., Critser, J.K., Cuppen, E., Dominiczak, A., Fernandez-Suarez, X.M., Flint, J., Gauguier, D., Geurts, A.M., Gould, M., Harris, P.C., Holmdahl, R., Hubner, N., Izsvak, Z., Jacob, H.J., Kuramoto, T., Kwitek, A.E., Marrone, A., Mashimo, T., Moreno, C., Mullins, J., Mullins, L., Olsson, T., Pravenec, M., Riley, L., Saar, K., Serikawa, T., Shull, J.D., Szpirer, C., Twigger, S.N., Voigt, B., and Worley, K. 2008. Progress and prospects in rat genetics: a community view. *Nat. Genet.* 40: 516–522.
2. Baker, H.J., Lindsey, J.R., and Weisbroth, S.H. 1979. The Laboratory Rat, Academic Press, New York.
3. Beermann, F., Orlow, S.J., and Lamoreux, M.L. 2004. The Tyr (albino) locus of the laboratory mouse. *Mamm. Genome* 15: 749–758.
4. Blaszczyk, W.M., Arning, L., Hoffmann, K.P., and Epplen, J.T. 2005. A Tyrosinase missense mutation causes albinism in the Wistar rat. *Pigment Cell Res.* 18: 144–145.
5. Cooksey, C.J., Garratt, P.J., Land, E.J., Pavel, S., Ramsden, C.A., Riley, P.A., and Smit, N.P. 1997. Evidence of the indirect formation of the catecholic intermediate substrate responsible for the autoactivation kinetics of tyrosinase. *J. Biol. Chem.* 272: 26226–26235.
6. Erb, C. 2006. Embryology and teratology. pp. 817–846. *In*: The Laboratory Rat (Suckow, M.A., Weisbroth, S.H., and Franklin, C.L. eds.), Elsevier Academic Press, Burlington.
7. Friedman, J.M., Leibel, R.L., and Bahary, N. 1991. Molecular mapping of obesity genes. *Mamm. Genome* 1: 130–144.
8. Futaki, S., Takagishi, Y., Hayashi, Y., Ohmori, S., Kanou, Y., Inouye, M., Oda, S., Seo, H., Iwaikawa, Y., and Murata, Y. 2000. Identification of a novel myosin-Va mutation in an ataxic mutant rat, dilute-opisthotonus. *Mamm. Genome* 11: 649–655.
9. Gibbs, R.A., Weinstock, G.M., Metzker, M.L., Muzny, D.M., Sodergren, E.J., Scherer, S., Scott, G., Steffen, D., Worley, K.C., Burch, P.E., Okwuonu, G., Hines, S., Lewis, L., DeRamo, C., Delgado, O., Dugan-Rocha, S., Miner, G., Morgan, M., Hawes, A., Gill, R., Celera, Holt, R.A., Adams, M.D., Amanatides, P.G., Baden-Tillson, H., Barnstead, M., Chin, S., Evans, C.A., Ferriera, S., Fosler, C., Glodek, A., Gu, Z., Jennings, D., Kraft, C.L., Nguyen, T., Pfannkoch, C.M., Sitter, C., Sutton, G.G., Venter, J.C., Woodage, T., Smith, D., Lee, H.M., Gustafson, E., Cahill, P., Kana, A., Doucette-Stamm, L., Weinstock, K., Fechtel, K., Weiss, R.B., Dunn, D.M., Green, E.D., Blakesley, R.W., Bouffard, G.G., De Jong, P.J., Osoegawa, K., Zhu, B., Marra, M., Schein, J., Bosdet, I., Fjell, C., Jones, S., Krzywinski, M., Mathewson, C., Siddiqui, A., Wye, N., McPherson, J., Zhao, S., Fraser, C.M., Shetty, J., Shatsman, S., Geer, K., Chen, Y., Abramzon, S., Nierman, W.C., Havlak, P.H., Chen, R., Durbin, K.J., Egan, A., Ren, Y., Song, X.Z., Li, B., Liu, Y., Qin, X., Cawley, S., Worley, K.C., Cooney, A.J., D'Souza, L.M., Martin, K., Wu, J.Q., Gonzalez-Garay, M.L., Jackson, A.R., Kalafus, K.J., McLeod, M.P., Milosavljevic, A., Virk, D., Volkov, A., Wheeler, D.A., Zhang, Z., Bailey, J.A., Eichler, E.E., Tuzun, E., Birney, E., Mongin, E., Ureta-Vidal, A., Woodwark, C., Zdobnov, E., Bork, P., Suyama, M., Torrents, D., Alexandersson, M., Trask, B.J., Young, J.M., Huang, H., Wang, H., Xing, H., Daniels, S., Gietzen, D., Schmidt, J., Stevens, K., Vitt, U., Wingrove, J., Camara, F., Mar Alba, M., Abril, J.F., Guigo, R., Smit, A., Dubchak, I., Rubin, E.M., Couronne, O., Poliakov, A., Hubner, N., Ganten, D., Goesele, C., Hummel, O., Kreitler, T., Lee, Y.A., Monti, J., Schulz, H., Zimdahl, H., Himmelbauer, H., Lehrach, H., Jacob, H.J., Bromberg, S., Gullings-Handley, J., Jensen-Seaman, M.I., Kwitek, A.E., Lazar, J., Pasko, D., Tonellato, P.J., Twigger, S., Ponting, C.P., Duarte, J.M., Rice, S., Goodstadt, L., Beatson, S.A., Emes, R.D., Winter, E.E., Webber, C., Brandt, P., Nyakatura, G., Adetobi, M., Chiaromonte, F., Elnitski, L., Eswara, P., Hardison, R.C., Hou, M., Kolbe, D., Makova, K., Miller, W., Nekrutenko, A., Riemer, C., Schwartz, S., Taylor, J., Yang, S., Zhang, Y., Lindpaintner, K., Andrews, T.D., Caccamo, M., Clamp, M., Clarke, L., Curwen, V., Durbin, R., Eyras, E., Searle, S.M., Cooper, G.M., Batzoglou, S., Brudno, M., Sidow, A., Stone, E.A., Venter, J.C., Payseur, B.A., Bourque, G., Lopez-Otin, C., Puente, X.S., Chakrabarti, K., Chatterji, S., Dewey, C.,